

# 1 Dangerous degree forecast of soil and water loss on highway slopes in 2 mountainous areas using RUSLE model

3 Yue Li<sup>1,2</sup>, Shi Qi<sup>\*1,2</sup>, Bin Liang<sup>1,2</sup>, Junming Ma<sup>1,2</sup>, Baihan Cheng<sup>1,2</sup>, Cong Ma<sup>3</sup>, Yidan Qiu<sup>3</sup>,  
4 and Qinyan Chen<sup>3</sup>

5 <sup>1</sup> Key Laboratory of State Forestry Administration on Soil and Water Conservation, Beijing  
6 Forestry University, Beijing 100083, China

7 <sup>2</sup> Beijing Engineering Research Center of Soil and Water Conservation, Beijing Forestry  
8 University, Beijing 100083, China

9 <sup>3</sup> Yunnan Science Research Institute of Communication & Transportation, Kunming 650011,  
10 China

## 11 **Abstract**

12 Many high and steep slopes are formed by special topographic and geomorphic types and  
13 mining activities during the construction of mountain expressways. Severe soil erosion may occur  
14 under heavy rainfall conditions. Therefore, predicting soil and water loss on highway slopes is  
15 important in protecting infrastructure and human life. This work studies Xinhe Expressway, which  
16 is in the southern edge of Yunnan–Guizhou Plateau, as the research area. The revised universal  
17 soil loss equation is selected as the prediction model of the soil and water loss on the slopes.  
18 Moreover, geographic information system, remote sensing technology, field survey, runoff plot  
19 observation testing, cluster analysis, and cokriging are adopted. The partition of the prediction  
20 units of the soil and water loss on the expressway slope in the mountain area and the spatial  
21 distribution model of the linear highway rainfall are studied. In view of the particularity of the  
22 expressway slope in the mountain area, the model parameter factor is modified and the risk of soil  
23 and water loss along the mountain expressway is simulated and predicted under 20- and 1-year  
24 rainfall return periods. The results are as follows. (1) Considering natural watershed as the  
25 prediction unit of slope soil erosion can represent the actual situation of the soil and water loss of  
26 each slope. The spatial location of the soil erosion unit is realized. (2) An analysis of the actual  
27 observation data shows that the overall average absolute error of the monitoring area is 33.24  
28  $t \cdot km^{-2} \cdot a^{-1}$ , the overall average relative error is 33.96%, and the overall root mean square error is  
29 between 20.95 and 65.64, all of which are within acceptable limits. The Nash efficiency  
30 coefficient is 0.67, which shows that the prediction accuracy of the model satisfies the  
31 requirements. (3) Under the condition of 1-year rainfall, we find through risk classification that the  
32 percentage of prediction units with no risk of erosion is 78%. Results show that soil erosion risk is  
33 low and therefore does not affect road traffic safety. Under the 20-year rainfall condition, the  
34 percentage of units with high risk and extremely high risk is 7.11% and mainly distributed on the  
35 K109+500–K110+500 and K133–K139+800 sections. The prediction results can help adjust the  
36 layout of the water and soil conservation measures in these units.

39 **Key words:** Soil and water loss; highway slopes; mountainous areas; RUSLE;  
40 dangerous degree forecast

41

## 42 **Introduction**

43 China has been gradually accelerating the construction of highways in recent years, thereby  
44 improving the transportation network and driving rapid economic development. Especially with  
45 the implementation of the western development strategy of the country, advanced requirements  
46 that focus on gradually connecting coastal plains and inland mountains have been proposed for the  
47 construction of expressways. Many unstable high and steep slopes, such as natural, excavation,  
48 and fill slopes, are inevitably formed by the considerable filling and deep digging along  
49 expressways in mountain areas.

50 The slope is the most fragile part of an expressway in a mountain area. During the rainy  
51 season, soil erosion is easily caused by rainwash and leads to a worrisome extent of damage  
52 (Figure 1). At present, China's highway industry is still in a period of rapid development. By the  
53 end of 2014, the total mileages of highway network exceeds 4,400,000 kilometers, and the  
54 expressway's mileage is 112,000 kilometers (Yuan et al., 2017; Mori et al., 2017; Kateb et al.,  
55 2013; Zhou et al., 2016). According to statistics, with the development of highway construction in  
56 China, slope areas reach 200–300 million m<sup>2</sup> each year (Dong and Zeng 2003). In the next 20–30  
57 years, expressways in China will measure more than 40,000 km. For every kilometer of a highway,  
58 the corresponding bare slope area formed measures 50,000–70,000 m<sup>2</sup>. The annual amount of soil  
59 erosion is 9,000 g/m<sup>2</sup>, which causes 450 t of soil loss every year (Chen 2010). **The soil and water  
60 loss of roadbed slope is different from that of soil and water in woodland and farmland.**  
61 Forestlands and farmlands are generally formed after years of evolution and belong to the native  
62 landscape. Most slopes are gentle and stable (Kateb et al., 2013). **Traditional soil and water  
63 conservation research focus on slopes with 20% grade or below, but the roadbed slope of the  
64 highway is generally greater than 30% (Zhou 2010).** Soil erosion on roadbed side slopes affects  
65 not only soil and water loss along the highway but also road operation safety (Gong and Yang  
66 2016; Jiang et al., 2017). Therefore, soil erosion on the side slopes of mountain expressways must  
67 be studied to control soil erosion, improve the ecological environment of expressways, and realize  
68 sustainable land utilization (Wang et al., 2005; Yang and Wang 2006).

69 **RUSLE is a set of mathematical equations that estimate average annual soil loss and  
70 sediment yield resulting from interrill and rill erosion (Renard et al., 1997; Foster et al., 1999;  
71 Zerihun et al., 2018; Toy et al., 2002). It is derived from the theory of erosion processes, more  
72 than 10,000 plot-years of data from natural rainfall plots, and numerous rainfall-simulation plots.  
73 RUSLE is an exceptionally well-validated and documented equation. A strength of RUSLE is that  
74 it was developed by a group of nationally-recognized scientists and soil conservationists who had  
75 considerable experience with erosional processes. (Soil and Water Conservation Society, 1993).**

76 The use of revised universal soil loss equation (RUSLE) models as predictive tools for the  
77 quantitative estimation of soil erosion has been maturing for a long time (Panagos et al., 2018;

78 Cunha et al., 2017; Taye et al., 2017; Renard 1997). The range of application of these models  
79 involves nearly every aspect of soil erosion. Moreover, many scholars have made many useful  
80 explorations in modifying the model parameter values and improving the simulation accuracy:

81 Tresch et al. (1995) believed that the slope length ( $L$ ) or slope steepness factor ( $S$ ) is one of  
82 the main factor for soil erosion prediction, and significantly influence the erosion values  
83 calculated by the RUSLE. All existing  $S$  factors are derived only from gentle slope inclinations of  
84 up to 32%. Many cultivated areas, particularly in Switzerland, are steeper than this critical value.  
85 Eighteen plot measurements on transects along slopes ranging from 20–90% in steepness were  
86 used in this study to qualitatively assess the most suitable  $S$  factors for steep subalpine slopes.  
87 Results showed that a first selection of an  $S$  factor was possible for slopes above the critical 25%  
88 steepness (Tresch et al., 1995). Rick D (2001) found that using universal soil loss equation (USLE)  
89 and RUSLE soil erosion models at regional landscape scales is limited by the difficulty of  
90 obtaining an  $LS$  factor grid suitable for use in geographic information system (GIS) applications.  
91 Therefore, he described the modifications applied to the previous arc macro language (AML) code  
92 to produce a RUSLE-based version of the  $LS$  factor grid. These alterations included replacing the  
93 USLE algorithms with their RUSLE counterparts and redefining assumptions on slope  
94 characteristics. Finally, in areas of western USA where the models were tested, the RUSLE-based  
95 AML program produced  $LS$  values that were roughly comparable to those listed in the RUSLE  
96 handbook guidelines (Rick et al., 2001). Silburn's (2011) research showed that estimating  $K$  from  
97 soil properties (derived from cultivated soils) provided a reasonable estimate of  $K$  for the main  
98 duplex soils at the study site as long as the correction for the undisturbed soil was used to derive  $K$   
99 from the measured data and to apply the USLE model (Silburn 2011). Wu (2014) adopted GIS and  
100 Revised Universal Soil Loss Equation (RUSLE) method to analyze the risk pattern of soil erosion  
101 in the affected road zone of Hangjinqi highway in Zhuji City, Zhejiang Province. Digital  
102 Elevation Model (DEM) data, rainfall records, soil type data, remote sensing imaging, and a road  
103 map of Hangjinqi highway were used for these GIS and RUSLE analyses (Wu et al., 2014). Chen  
104 (2010) according to terrain characteristics of roadbed side slope and through concrete analysis of  
105 terrain factor calculation method in Revised Universal Soil Loss Equation (RUSLE), the  
106 compatible question of terrain factor computational method of roadbed side slope is appraised and  
107 the revision method on the basis of measured data of soil erosion in subgrade side slope of  
108 Hurongxi Expressway (from Enshi to Lichuan) in Hubei Province is proposed. The results indicate

109 that: (1) In RUSLE slope length factor can be calculated by formula of  $L = \left(\frac{\lambda}{22.1}\right)^m$ , but  $m$   
110 should not be checked by the original method for the highway subgrade side slope because its  
111 gradient surpasses generally applicable scope of RUSLE; (2)  $L$ , slope length factor of highway

112 subgrade side slope can be calculated by formula  $L = \left(\frac{\lambda}{22.1}\right)^{0.35}$  (Chen et al., 2010). Zhang (2016)  
113 investigated the spatio-temporal distribution of soil erosion in ring expressway before and after  
114 construction process, they used land use/cover map of Ningbo City in 2010, topographic map,

115 map of North Ring expressway and field survey data was collected to derive digital elevation  
116 model (DEM). Rainfall data was collected from local hydrological station. Based on the collected  
117 data, the spatial distribution of the factors in RUSLE model was calculated, and soil erosion maps  
118 of the north ring expressway were estimated. Then, the soil erosion amount was calculated at three  
119 different stages by using RUSLE model. The results shows that: Slight erosion was dominant  
120 during preconstruction period and natural recovery period, which accounted for 98.53% and  
121 99.73%, respectively. During construction period, mild erosion and slight erosion was the largest,  
122 which accounted for 52.5% and 35.4%, respectively. In general, soil erosion during the  
123 construction period is mainly distributed in the temporary soil ground (Zhang et al., 2016).

124 However, methods used to fit the parameters affected the results, and minimizing the sum of the  
125 squares of errors in the soil losses provided better results than fitting an exponential equation did.  
126 Yang (2014) found that the *C* factor value can be determined as a function of fractional bare soil  
127 and ground cover derived from MODIS data at regional or catchment scales. The method offers a  
128 meaningful estimate of the *C* factor, thus indicating ground cover impact on soil loss and erosion  
129 hazard areas. The method is better than the commonly used techniques, which are based only on  
130 green vegetation (e.g., normalized difference vegetation index, NDVI). Thus, the study provided  
131 an appropriate approach to estimating the *C* factor in hillslope erosion modeling in New South  
132 Wales, Australia, using emerging fractional vegetation cover products. This approach simply and  
133 effectively mapped the spatial and temporal distribution of the RUSLE cover factor and hillslope  
134 erosion hazard in a large area. The methods and results described in this article are valuable for  
135 understanding the spatial and temporal dynamics of hillslope erosion and ground cover.  
136 According to a study by Kinnell PIA (2014), runoff production, which is spatially uniform, is  
137 often inappropriate under natural conditions, where infiltration is spatially variable. The use of an  
138 upslope slope length that varies with the ratio of the upslope runoff coefficient to the runoff  
139 coefficient for the area down to the downslope boundary of the segment in modifications of the  
140 RUSLE approach produces only minor variations in soil loss compared with those predicted using  
141 the standard RUSLE approach when the runoff is spatially variable and the number of segments  
142 increases. On the contrary, the USLE-M approach provides predictions of soil loss that are  
143 influenced strongly by runoff when runoff varies in space and time. Therefore, an increase in the  
144 runoff through a segment causes an increase in soil loss, whereas a decrease in the runoff through  
145 a segment or cell results in a decrease in soil loss.

146 In general, these studies are mainly limited to sloping fields (Tresch S and others 1995; Rick  
147 D and others 2001; Silburn 2011; Yang 2014; Kinnell 2014).The research on soil erosion on  
148 highway slopes is limited. Subgrade slope is a major part of soil erosion in construction and  
149 operation periods. Therefore, the soil erosion caused by this slope should be predicted. **However,**  
150 **the research progress on soil and water loss of highway hardly meet the requirements of the**  
151 **practical work. (Xu et al., 2009; Bakr et al., 2012). So far, we still need to do a lot of work on the**  
152 **prediction of soil erosion in highway slopes.** The situation in various regions in China shows that  
153 certain researchers have improved the RUSLE model and studied soil erosion that occurs in

154 certain areas. Water and soil erosion caused by engineering construction is an important form after  
155 agricultural cultivation and forestry deforestation, the amount of soil erosion produced by the  
156 embankment slope occupies a large proportion in the whole project. It is not only related to the  
157 feasibility and cost of the project, but also has aroused great interest and attention. Yang (2001)  
158 investigated the behavior of soil erosion on the slope of a railway embankment during  
159 construction by comparing artificial and natural rainfalls on the special Qinhuangdao–Shenyang  
160 line of passenger trains. The results showed that the main type of soil erosion in the study area was  
161 gully erosion, which caused more soil erosion than surface erosion did; in addition, the principal  
162 factor causing soil erosion on the slope was the amount of precipitation and the width of the  
163 embankment. Wang (2005) established several experimental standardized spots for soil loss  
164 collection on the side slopes of the Xiaogan–Xiang fan freeway under construction and installed  
165 an on-the-spot auto-recorder of rainfall. The data collected were used for the revision of the main  
166 parameters  $R$  (rainfall and runoff) and  $K$  (erodibility of soil) of the USLE, which is widely applied  
167 to forecast soil loss quantity in plowlands and predict the soil loss quantities of different types of  
168 soil on side slopes disturbed by engineering treatment (Wang et al., 2005). It can not only be  
169 applied to the prediction of disturbed soil loss in expressway construction, but also improve the  
170 prediction accuracy. It provides scientific support for relevant units or personnel to take reasonable  
171 preventive measures.

172 According to the literature, the study of soil and water loss in highways has the following  
173 problems. (1) In using the RUSLE model, most of the research on the  $C$  and  $P$  factors was  
174 conducted by referring to previous research results and data accuracy is often poor. (2) Most  
175 studies on rainfall erosivity ( $R$ ) factors are still limited to sloping fields, and the rainfall erosivity  
176 factors of expressway slopes in mountain areas have rarely been studied. (3) Slope soils in  
177 highways differ from the broad sense of arable soil; moreover, the slopes themselves are also  
178 varied. Thus, accurately predicting the soil loss of different types of subgrade slopes using the  
179 traditional  $K$  factor calculation method is difficult.

180 Therefore, the RUSLE equation is selected as the prediction model for the soil and water loss  
181 on slopes with GIS technology as support in view of the characteristics of the soil and water loss  
182 in mountain expressways. The soil erodibility factor ( $K$ ), slope length factor ( $LS$ ), and soil and  
183 water conservation measure factor ( $P$ ) are revised to improve the method of dividing slope units.  
184 In determining the predictive parameters of the model, the **rainfall** is obtained by spatial  
185 interpolation. The use of this technique addresses the shortage of rainfall data in mountain areas,  
186 the difficulty of representing the rainfall data of an entire expressway with those from a single  
187 meteorological station, and the uneven spatial distribution and strong heterogeneity of rainfall in  
188 mountain areas. In this study, a suitable prediction model of soil and water loss is established, the  
189 parameters of the model are revised, and the risk of soil and water loss under different rainfall  
190 scenarios is simulated and predicted. **This study not only scientifically predicts the amount of soil  
191 erosion caused by the highway construction in mountain areas, but also provides a scientific basis  
192 for the prevention and control of soil erosion, and the rational allocation of prevention and control**

193 **measures.** Meanwhile, the safe operation of highways and the virtuous cycle of the ecological  
194 environment should be ensured to promote the sustainable development of the local economy.

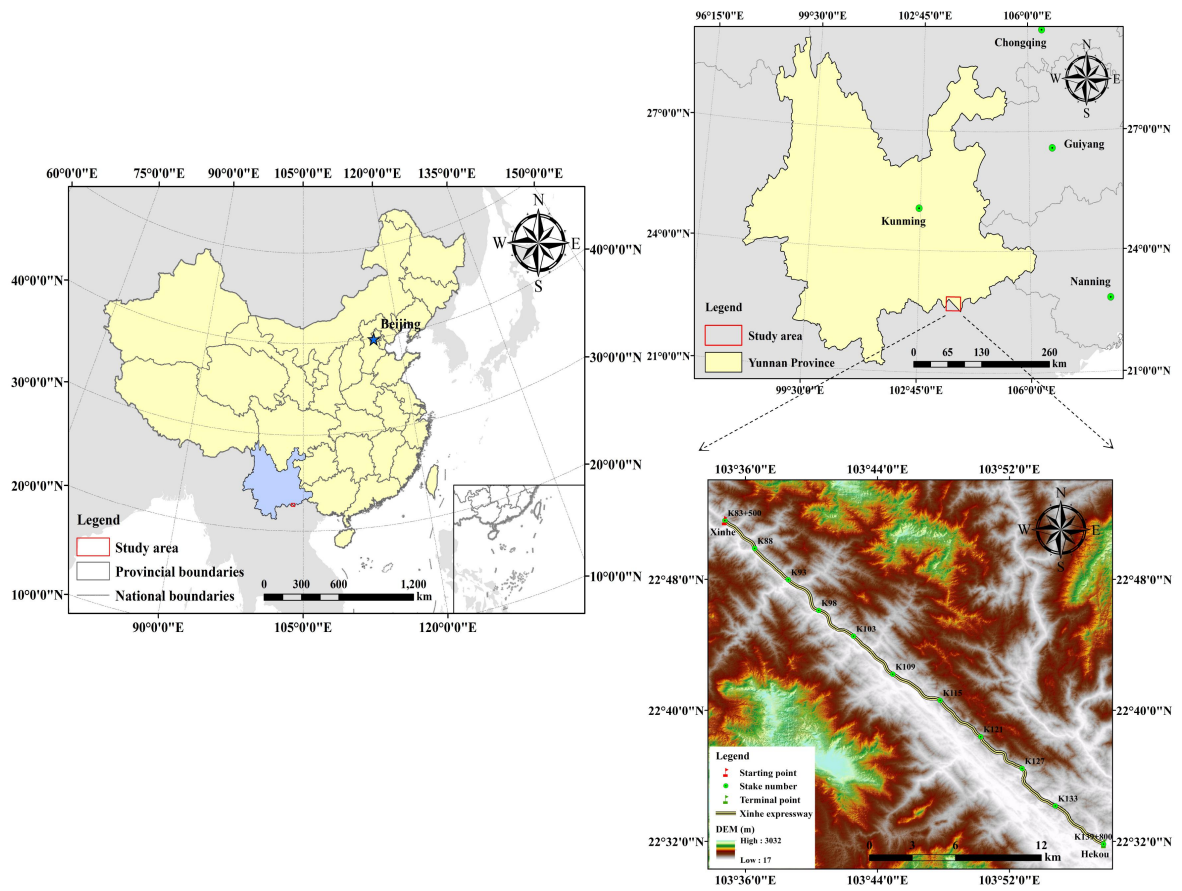
## 195 **1 Study area**

196 Xinhe Expressway is in the southern margin of the Yunnan–Guizhou Plateau, which is in  
197 southeast Yunnan Province, Honghe Prefecture, and Hekou County. This highway was the first in  
198 Yunnan to cross the border, thereby becoming an important communication channel between  
199 China and Vietnam and obtaining important strategic and economic value. The highway is at  
200 longitude 103° 33' 45"–103° 58' 32" and latitude 22° 31' 19"–22° 51' 48". The expressway  
201 stretches roughly from northwest to southeast, and the total length is 56.30 km. The climate type  
202 belongs to subtropical mountain, seasonal monsoon forest, and humid heat climate categories.  
203 **Between May and the middle of October, the area experiences wet season characterized by**  
204 **abundant rainfall, concentrated precipitation, and increased rain at night, the variation on**  
205 **precipitation is from 400 to 2000mm, and most of the regions are between 800 to 1800mm (Fei et**  
206 **al., 2017; Zhang et al., 2017).** During the rest of the year, the area undergoes dry season. The  
207 starting point of Xinhe Expressway is in Hekou County, New Street (pile number K83+500) at an  
208 altitude of 296 m. The end point is in the estuary of Areca Village (pile number K139+800) at an  
209 altitude of 95 m. The mountains along both sides are 200–380 m above sea level (Figure 2). The  
210 topography of the hilly area in the northern part of Xinhe Expressway is complicated. The slopes  
211 on both sides rise and fall, and most of the valleys constitute “V”- and “U”- shaped sections. The  
212 natural slopes on both sides are mostly below 30°. The southern part of the highway has a  
213 relatively flat terrain and a gentle slope. The slope of most of the hills on both sides is less than  
214 15°, and the overall height difference is smaller than 100 m. The vegetation in the southern part of  
215 Xinhe Expressway includes tropical rainforests and tropical monsoon forests. Meanwhile, the  
216 vegetation in the northern part of China is classified as a south subtropical monsoon evergreen  
217 broad-leaved forest. In recent years, the original vegetation in this area has been reclaimed as  
218 farmland and is now planted with rubber, banana, pineapple, and pomegranate, which are sporadic  
219 tropical rainforest survivors. The project area along Xinhe Expressway is an economic forest belt  
220 with a single vegetation type and mainly has rubber, forest, and other economic trees. The soil  
221 types along the highway are rich and mainly red, leached cinnamon, gray forest, and gray  
222 cinnamon soils.



223  
224  
225

Figure 1. Soil erosion produced by rainwash on slope



226  
227

Figure 2. Overview of study region

## 228 **2 Materials and method**

### 229 **2.1 Data sources**

#### 230 2.1.1 Meteorological data

231 Rainfall data from 2014 were obtained from Hekou Yao Autonomous County, Pingbian Miao  
232 Autonomous County, Jinping Miao Yao Autonomous County, and the meteorological department  
233 of Mengzi. The rainfall data type was in 5 min format. Meanwhile, two automatic weather stations  
234 were established along Xinha Expressway to gather weather data during the 2014 experiment.  
235 Meteorological data was provided by the China Meteorological Data Network covered the period  
236 of 1959–2015 (<http://data.cma.cn/site/index.html>).

#### 237 2.1.2 Soil data

238 Soil type data were provided by Yunnan Traffic Planning and Design Institute. Soil texture  
239 and organic matter data were obtained by field surveys, data sampling, and processing methods.  
240 Soil samples were collected from every 1 km of the artificial and natural slopes on both sides of  
241 the highway. Five mixed soil samples were obtained from one slope using the “S”-shaped  
242 sampling method (Shu et al., 2017). Then, **the method of coning and quartering** was adopted  
243 (Oyekunle et al., 2011), and half of the soil samples from the mixed soil samples were brought to  
244 the laboratory for analysis. Finally, 186 soil samples were obtained. After the soil samples were  
245 dried and sieved, we measured the soil texture and organic carbon content through specific gravity  
246 speed measurement and potassium dichromate external heating, respectively.

#### 247 2.1.3 Topographic data

248 A topographic map and design drawings of Xinha Expressway were provided by the Traffic  
249 Planning and Design Institute of Yunnan Province. The 1:2000 scale of the topographic map  
250 coordinate system was based on the 2000 GeKaiMeng urban coordinate system, elevation system  
251 for the 1985 national height datum, and the format for the CAD map DWG format.

#### 252 2.1.4 Image data

253 The remote sensing images used in this study were derived from 8m hyperspectral images  
254 produced by GF-1 satellite (<http://www.rscloudmart.com/>).

255

### 256 **2.2 Predicting model selection**

257 The RUSLE equation (Renard et al., 1997) was used to predict the soil and water loss on the  
258 side slopes of Xinha Expressway. The RUSLE equation considers natural and anthropogenic  
259 factors that cause soil erosion to produce comprehensive results. Various parameters are easy to  
260 calculate, and the calculation method is relatively mature. The RUSLE model is suitable for soil  
261 erosion prediction in areas where the physical model is not needed. See Formula (1).

$$262 \quad A = R \cdot K \cdot L \cdot S \cdot C \cdot P, \quad (1)$$

263 where  $A$  is the average soil loss per unit area by erosion ( $t/hm^2$ ),  $R$  is the rainfall erosivity factor  
264 ( $MJ \cdot mm / (hm^2 \cdot h)$ ),  $K$  is the soil erodibility factor ( $t \cdot hm^2 \cdot h / (hm^2 \cdot MJ \cdot mm)$ ),  $L$  is the slope length  
265 factor,  $S$  is the steepness factor,  $C$  is the cover and management practice factor, and  $P$  is the



266 conservation support practice factor. The values of  $L$ ,  $S$ ,  $C$ , and  $P$  are dimensionless.

267

### 268 2.3 Prediction unit division and implementation

269 Geological structures and rock and soil categories are complex because of considerable  
270 changes in topography and physiognomy. The forms of slopes also vary. In general, according to  
271 the relationship between slope and engineering, slopes can be natural or artificial. Artificial slope  
272 formations can be subdivided into slope embankments and cutting slopes. This study used the  
273 software ArcGIS to convert the topographic map of the highway design into a vectorization file  
274 because the artificial and natural slopes of watershed catchments are the main components of soil  
275 erosion prediction. **On the basis of the extracted graphical units of the artificial and natural slope,**  
276 **the natural and artificial slope was divided into a uniform prediction unit according to the aspect,**  
277 **slope, land use, water conservation measures.** The aspect, slope, land use, water conservation  
278 measures, and other attributes of each prediction unit were consistent.

279

## 280 3 Results and analysis

### 281 3.1 Natural slope catchment area

282 The catchment unit of the slope was constructed using the structural plane tools of ArcGIS  
283 combined with ridge and valley lines and artificial slope and highway boundaries (Zerihun et al.,  
284 2018). After the completion of the catchment unit, the slope was divided according to soil type  
285 data (Table 1). After the division and overlaying of the remote sensing image map, the land use  
286 types and soil and water conservation measures were considered indicators through visual  
287 interpretation and field survey results in further classifying the confluence units. Finally, the  
288 partition units were amended using the vegetation coverage data obtained along Xinhe  
289 Expressway. A total of 814 natural slope catchment prediction units were divided.

290

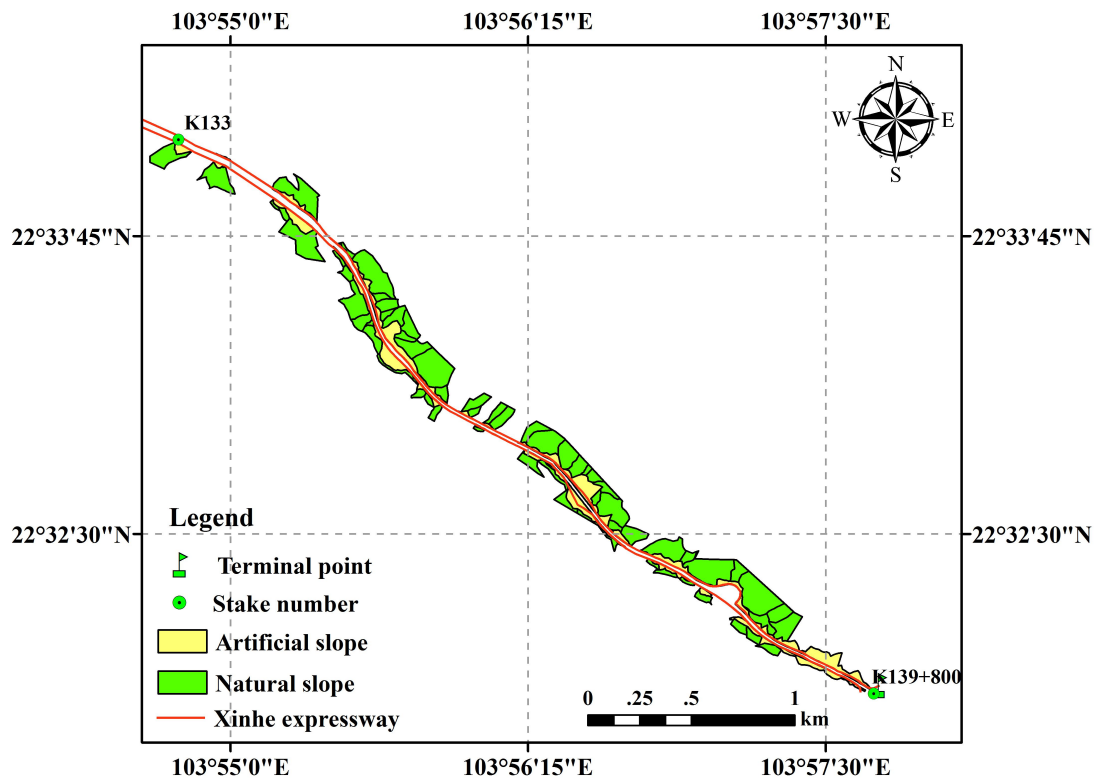
291 **Table 1.** Distribution of soil types along Xinhe Expressway

A section of a expressway	Soil type
K83+500~K84+900	latosolic red soil
K85+200~K93+200	leached cinnamon soil
K93+200~K95+900	gray forest soil
K96+900~K97+800	gray cinnamon soil
K97+800~K100+500	leached cinnamon soil
K100+500~K101+100	gray cinnamon soil
K101+100~K104	leached cinnamon soil
K104~K109+100	gray cinnamon soil
K109+100~K139	leached cinnamon soil

292

293 The artificial slope was divided into roadbed and cutting slopes according to the design of  
294 Xinhe Expressway into 1:1.5 and 1:1.0 slopes. After the preliminary division, the slope  
295 measurements, data design, and field survey results were used as bases for the subsequent detailed  
296 division of the artificial slope into cement frame protection and six arris brick revetments. **Mccool**  
297 **(1987) stated that slope length varies within a 10 m range and has only a small effect on results.**  
298 The specifications of each frame in the cement frame protection along Xinhe Expressway are the  
299 same. The horizontal projection length of the cement frame is the slope length value of the  
300 artificial slope. Therefore, the slope length of the artificial slope of each frame of the cement  
301 revetment was considered the same and with a value of 0. According to investigations, the  
302 vegetation coverage of artificial slopes with different plant species substantially varies. To achieve  
303 an accurate prediction of unit division and improve prediction accuracy, the artificial slopes should  
304 be continuously classified according to the plant species. A total of 422 artificial slope prediction  
305 units were thus obtained. Then, the data of the 1236 slope prediction units were edited using GIS.  
306 The results are shown in Figure 3.

307



308

309

**Figure 3. Division results of prediction units (A subset-6.8 km)**

310

### 311 3.2 Determination of conventional parameter factor values of RUSLE model

#### 312 3.2.1 Rainfall erosivity factor (*R*) (Panagos et al., 2017)

313 The formula of the *R* value (rainfall erosivity) was adopted (Wang et al., 1995; Liu et al.,  
314 1999; Yang et al., 1999). This value was calculated using 30 min rainfall intensity as a measure, as

315 shown by Formulas (2) and (3).

316 
$$R = 1.70 \cdot (P \cdot I_{30} / 100) - 0.136 \quad (I_{30} < 10 \text{ mm/h}), \quad (2)$$

317 
$$R = 2.35 \cdot (P \cdot I_{30} / 100) - 0.523 \quad (I_{30} \geq 10 \text{ mm/h}), \quad (3)$$

318 where  $R$  is the rainfall erosivity,  $P$  is the sub-rainfall, and  $I_{30}$  is the maximum 30 min rainfall  
319 intensity.

320 The rainfall data were acquired from stationary ground meteorological stations. Thus, using  
321 data from a single meteorological station to represent the rainfall data of a linear mountain  
322 expressway was difficult. The  $P$  and  $I_{30}$  values along the highway were obtained by the method of  
323 co-kriging calculations. The data included those derived from rainfall and 30 min rainfall data  
324 from four meteorological stations in Hekou Yao Autonomous County, Pingbian Miao Autonomous  
325 County, Jinping Miao Yao Autonomous County, and Mengzi City and those acquired from two  
326 automatic weather stations along the highway. Then, the cross-validation method was used to  
327 evaluate the accuracy of the interpolation results. The selection criteria were standard root mean  
328 square error and the mean standard error. Detailed results are shown in Table 2. This work shows  
329 only the interpolated results of secondary rainfall of two rainfall and 30 min rainfall intensity data,  
330 as shown in Figure 4(a) and Figure 4(b).

331

**Table 2.** Interpolation error of  $P$  and  $I_{30}$  values

The time of the second rainfall	$P$		$I_{30}$	
	RMSS	MS	RMSS	MS
2014.06.05	1.02	-0.02	1.06	-0.05
2014.06.07	1.04	-0.02	1.01	0.02
2014.06.17	1.09	0.03	1.11	0.06
2014.06.28	1.11	0.07	1.05	-0.03
2014.07.01	1.10	0.04	1.06	-0.04
2014.07.13	1.03	-0.02	1.01	0.02
2014.07.20	1.01	0.01	1.05	0.02
2014.08.02	1.03	0.03	0.94	0.02
2014.08.12	1.05	-0.03	1.10	0.03
2014.08.26	1.03	0.01	0.97	0.03
2014.08.29	1.09	-0.02	1.03	-0.02
2014.09.02	1.07	0.03	1.05	0.02
2014.09.04	0.96	-0.02	0.97	-0.02
2014.09.17	1.07	-0.03	1.09	-0.03
2014.09.20	0.98	0.05	1.03	0.02
2014.10.05	1.02	0.03	1.04	0.03

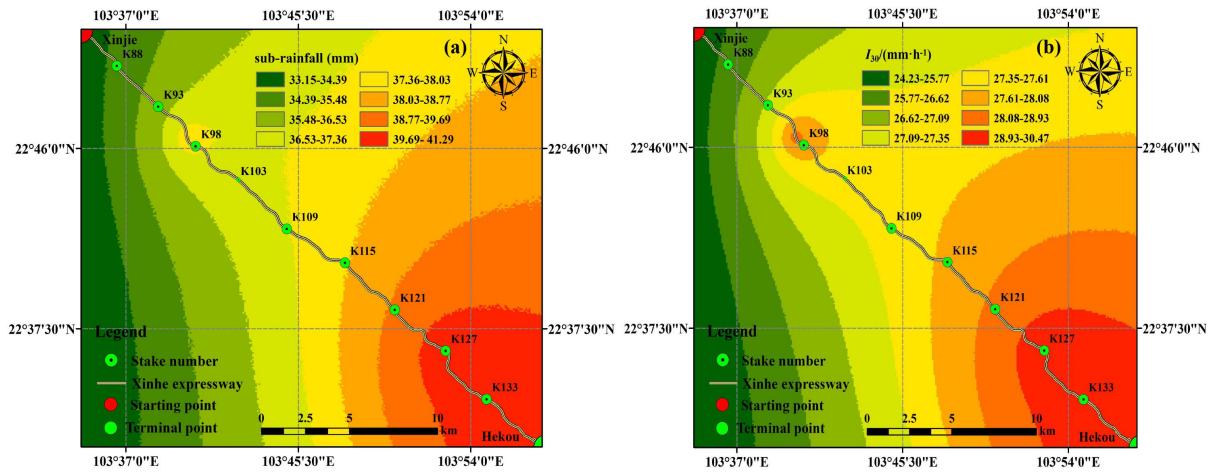


Figure 4(a). Interpolation results of secondary rainfall for June 5, 2014;

Figure 4(b). Interpolation results of  $I_{30}$  for June 5, 2014

The secondary rainfall data of 16 rainfall instances along Xinhe Expressway were obtained by interpolation because the internal rainfall and rainfall intensity of a single prediction unit are the same. Therefore, the  $R$  value was calculated using the average rainfall and rainfall intensity of the unit. Only the spatial distribution map of the rainfall erosivity factors in certain sections (June 5, 2014) is shown due to space constraints (Figure 5 and Figure 5a).

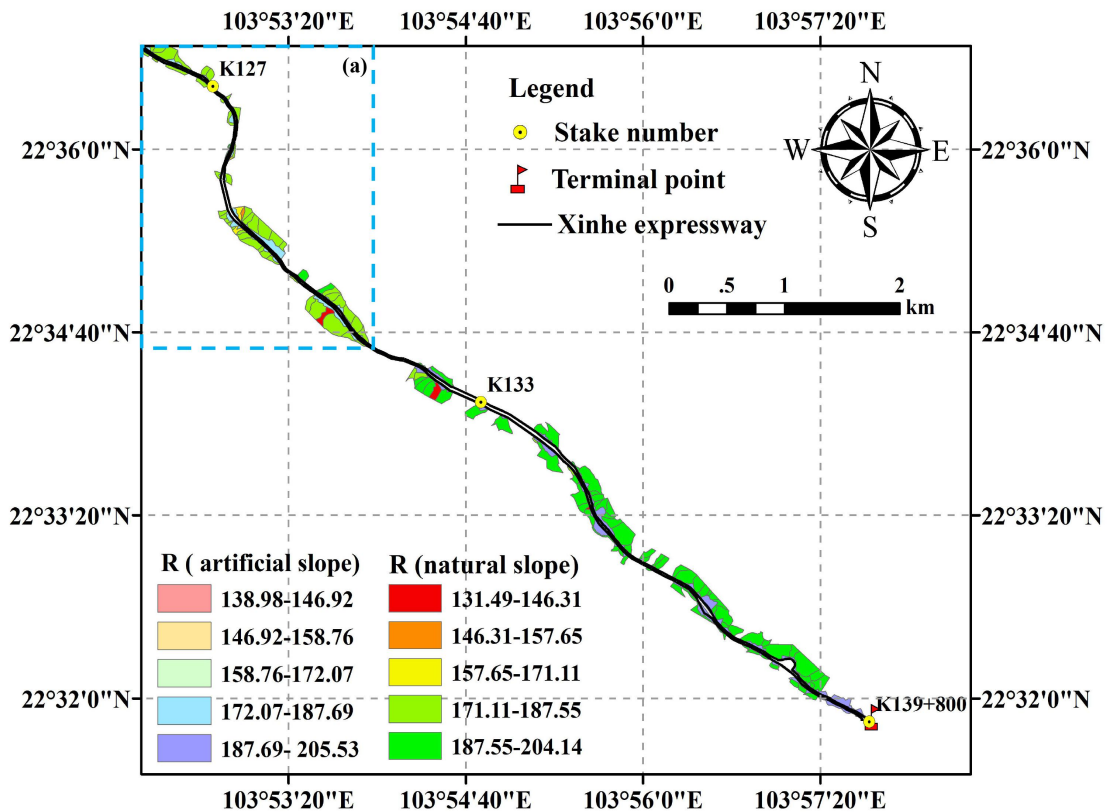


Figure 5. Spatial distribution map of rainfall erosivity factors (K127–K139+800)

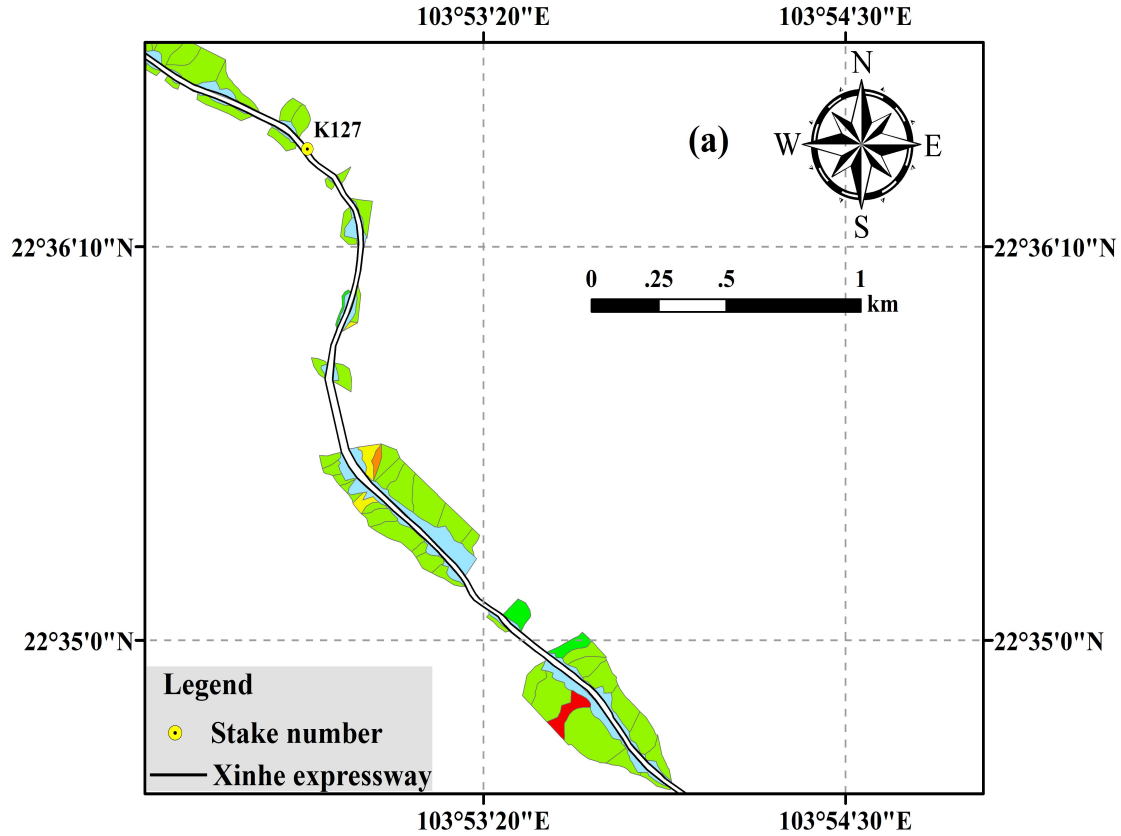


Figure 5(a). The subgraph of Figure 5 with zoomed sections.

344

345

346

### 3.2.2 Soil erodibility factor ( $K$ )

348

The soil data of the slope in each section were obtained by sampling on the basis of the spatial distribution map of soil types in the study area and dividing the linear distribution of the soil. The calculation method of the  $K$  value was adopted by Formula 4 to obtain the soil erodibility factor values of each slope (Sharply and Williams 1990 ), as shown in Tables 3 and 4 (see the supplementary material/appendices).

349

350

351

352

$$K = 0.2 + 0.3e^{[0.0256SAN(1-SIL/100)]} \times \left( \frac{SIL}{CLA + SIL} \right)^{0.3} \times \left[ 1 - \frac{0.25C}{C + e^{3.72-2.95C}} \right] \times \left[ 1 - \frac{0.75N_1}{SN_1 + e^{22.9SN_1-5.51}} \right] \quad (4)$$

354

In the formula, SAN, SIL, CLA, and C represent sand grains (0.05–2 mm), powder (0.002–0.05 mm), clay (<0.002 mm) and organic carbon content (%), and  $SN_1=1-SAN/100$ , respectively.

356

### 3.2.3 Calculation of topographic factors in natural slope catchments

358

#### (1) Slope length factor

359

According to the topographic map (1:2000 scale) and highway design of Xinhe Expressway, the slope length and factor of slope catchment were calculated using DEM data with 0.5 m spatial resolution generated by ArcGIS. The natural slope catchment slope was divided into less than  $1^\circ$ ,  $1^\circ-3^\circ$ ,  $3^\circ-5^\circ$ , and greater than or equal to  $5^\circ$  using the Reclassify tool in ArcGIS. The operation

360

361

362

363 formula adopted the L factor algorithm of Moore and Burch (1986), as shown by Formulas (5) and  
 364 (6).

$$365 \quad L = \left( \frac{\lambda}{22.13} \right)^m \quad (5)$$

$$366 \quad \lambda = \text{flowacc} \cdot \text{cellsize} \quad (6)$$

367 In the formula,  $L$  is normalized to the amount of soil erosion along the slope length of 22.13 m,  $\lambda$   
 368 is the slope length,  $\text{flowacc}$  is the total pixel number of water flowing into the pixel that is higher  
 369 than the pixel, and  $\text{cellsize}$  refers to the DEM resolution size. The value is 0.5 m, and  $m$  is the  $LS$   
 370 factor. See Formula (7).

$$371 \quad m = \begin{cases} 0.2 & \theta < 1^\circ \\ 0.3 & 1^\circ \leq \theta < 3^\circ \\ 0.4 & 3^\circ \leq \theta < 5^\circ \\ 0.5 & \theta \geq 5^\circ \end{cases}, \quad (7)$$

372 where  $\theta$  is the slope.

373 (2) Slope factor

374 The  $S$  factor was calculated as follows. If the slope was less than  $18^\circ$ , then the formula of  
 375 McCool et al. (1987) was used. If the slope was greater than  $18^\circ$ , then the formula of Liu et al.  
 376 (1994) was adopted. See Formula (8).

$$377 \quad S = \begin{cases} 10.8 \cdot \sin \theta + 0.03 & \theta < 9^\circ \\ 16.8 \cdot \sin \theta - 0.05 & 9^\circ \leq \theta < 18^\circ \\ 21.9 \cdot \sin \theta - 0.96 & \theta \geq 18^\circ \end{cases} \quad (8)$$

378 The DEM data were processed by ArcGIS to obtain slope data. The slope values of each  
 379 prediction unit were extracted using the Zonal statistics tool. Through the classification tool in  
 380 ArcGIS, the slope of the highway slope catchment of Xinhe was divided into less than  $9^\circ$ ,  $9^\circ$ – $18^\circ$ ,  
 381 and greater than or equal to  $18^\circ$ .

382 The  $S$  values of the slope catchments under the three slope grade conditions were calculated by  
 383 combining Formula (8) and ArcGIS techniques. The  $LS$  values of the slope prediction units are  
 384 shown in Figure 6.

385

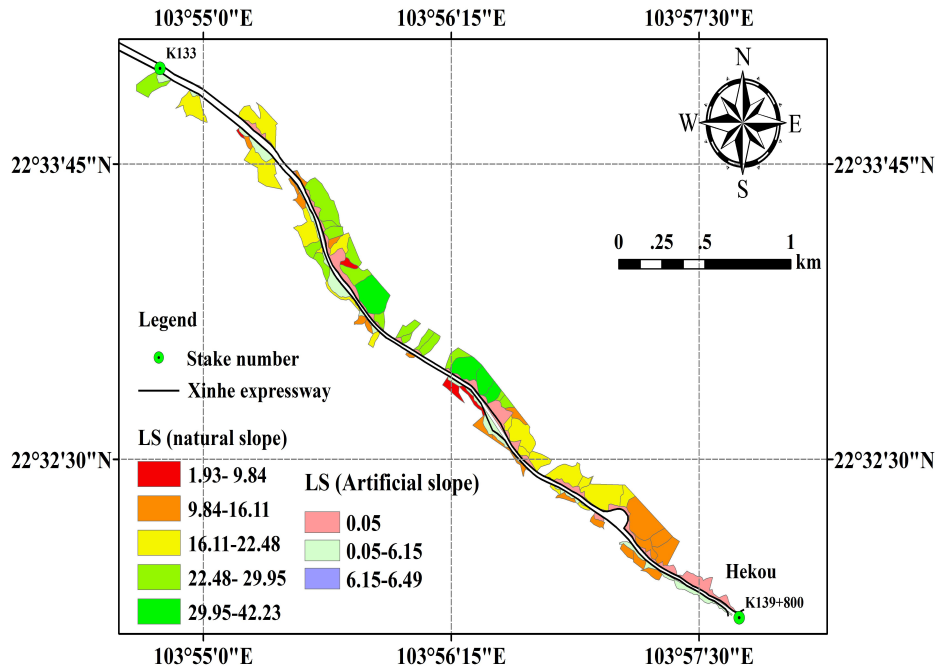


Figure 6. Spatial distribution map of topographic factors (K134–K139)

386  
387  
388

### 3.2.4 Calculation of topographic factors of artificial slopes

#### (1) Slope length factor

391 The method of Chen Zongwei (2010) was used to calculate the *LS* factor of the artificial slopes,  
392 and the calculation method for the topographic factors of the artificial slopes of Xinhe Expressway  
393 was modified. The slope length factor ( $L_a$ ) was calculated using Formulas (5) and (6). The slope  
394 length index ( $m_a$ ) was measured by a runoff plot experiment and then calculated by Formula (9).

$$395 \quad m_a = \log_{\frac{\lambda_1}{\lambda_2}} \frac{A_1}{A_2}, \quad (9)$$

396 where  $A_1$  and  $A_2$  are the soil erosion intensity values of two slopes when the slope lengths are  $\lambda_1$   
397 and  $\lambda_2$ , respectively. (The specifications of the two slopes were the same except for slope length.)  
398 The soil erosion amounts under 30 erosion rainfall conditions were monitored in the runoff field  
399 of Xiao Xinzhai of Mengzi City in 2014–2015 (Table 5). The  $m_a$  value under each rainfall  
400 condition was calculated using Formula (9) according to the monitoring value of soil erosion  
401 amount. The average value of  $m_a$  was 0.32, which was the  $m_a$  value of the artificial slope length  
402 factor, as shown in Table 6.

403

Table 5. Amount of soil erosion of monitoring areas ( $t \cdot km^{-2} \cdot a^{-1}$ )

The time of the second rainfall	1	2	3	4	5	6
2014.06.05	4212	5158	5922	6423	12896	888
2014.06.07	1997	2447	2812	3089	6170	426

2014.06.17	867	1098	1227	1341	2664	185
2014.06.28	5700	7128	8107	8979	17915	1225
2014.07.01	477	608	686	748	1498	103
2014.07.13	1560	1915	2159	2374	4757	327
2014.07.20	3857	4878	5617	6183	12323	849
2014.08.02	5601	7048	7939	8600	17231	1194
2014.08.12	1955	2491	2881	3148	6294	435
2014.08.26	6211	7630	8750	9561	19196	1315
2014.08.29	1539	1889	2161	2356	4701	326
2014.09.02	611	758	868	950	1910	131
2014.09.04	1487	1893	2172	2372	4761	324
2014.09.17	1577	1954	2250	2451	4809	336
2014.09.20	1076	1329	1512	1633	3252	224
2014.10.05	749	925	1064	1172	2356	160
2015.07.04	5216	6377	7260	7877	15653	1090
2015.07.15	1575	1925	2192	2416	4775	334
2015.07.24	991	1250	1394	1522	3002	212
2015.07.28	4200	5188	5907	6544	13005	886
2015.08.13	829	1057	1189	1292	2567	177
2015.08.19	1010	1233	1390	1521	3016	208
2015.08.26	1682	2108	2415	2673	5263	364
2015.09.03	386	481	543	583	1169	81
2015.09.12	591	745	857	940	1868	129
2015.09.17	1172	1433	1632	1789	3555	245
2015.09.25	1369	1690	1906	2089	4152	287
2015.10.03	1188	1468	1671	1832	3664	252
2015.10.08	2908	3707	4220	4599	9196	625
2015.10.12	779	963	1111	1215	2339	164

404

405

406

**Table 6.** Calculation results of  $m_a$

The time of the second rainfall	$m_{12}$	$m_{13}$	$m_{14}$	$m_{23}$	$m_{24}$	$m_{34}$
2014.06.05	0.29	0.31	0.30	0.34	0.32	0.28
2014.06.07	0.29	0.31	0.31	0.34	0.34	0.33
2014.06.17	0.34	0.32	0.31	0.27	0.29	0.31



2014.06.28	0.32	0.32	0.33	0.32	0.33	0.36
2014.07.01	0.35	0.33	0.32	0.30	0.30	0.30
2014.07.13	0.30	0.30	0.30	0.30	0.31	0.33
2014.07.20	0.34	0.34	0.34	0.35	0.34	0.34
2014.08.02	0.33	0.32	0.31	0.29	0.29	0.28
2014.08.12	0.35	0.35	0.34	0.36	0.34	0.31
2014.08.26	0.30	0.31	0.31	0.34	0.33	0.31
2014.08.29	0.30	0.31	0.31	0.33	0.32	0.30
2014.09.02	0.31	0.32	0.32	0.34	0.33	0.32
2014.09.04	0.35	0.35	0.34	0.34	0.33	0.31
2014.09.17	0.31	0.32	0.32	0.35	0.33	0.30
2014.09.20	0.30	0.31	0.30	0.32	0.30	0.27
2014.10.05	0.30	0.32	0.32	0.35	0.34	0.34
2015.07.04	0.29	0.30	0.30	0.32	0.30	0.29
2015.07.15	0.29	0.30	0.31	0.32	0.33	0.34
2015.07.24	0.33	0.31	0.31	0.27	0.28	0.31
2015.07.28	0.31	0.31	0.32	0.32	0.33	0.36
2015.08.13	0.35	0.33	0.32	0.29	0.29	0.29
2015.08.19	0.29	0.29	0.30	0.30	0.30	0.32
2015.08.26	0.33	0.33	0.33	0.34	0.34	0.36
2015.09.03	0.32	0.31	0.30	0.30	0.28	0.25
2015.09.12	0.34	0.34	0.34	0.35	0.34	0.32
2015.09.17	0.29	0.30	0.30	0.32	0.32	0.32
2015.09.25	0.30	0.30	0.30	0.30	0.31	0.32
2015.10.03	0.31	0.31	0.31	0.32	0.32	0.32
2015.10.08	0.35	0.34	0.33	0.32	0.31	0.30
2015.10.12	0.31	0.32	0.32	0.35	0.33	0.31
The average value of $m_a$				0.32		

407  $m_{xy}$  represents the  $m$  value simultaneously solved by erosion intensity values for monitoring plots that are  
408 numbered  $x$  and  $y$ .

409

410 (2) Slope factor

411 The calculation of slope factor was based on the research method of Chen Zongwei. Six runoff  
412 plots were established in the Xiao xinzhai runoff field of Mengzi City. The soil erosion intensity  
413 under slope conditions of 1:1.5, 1:1.0, and 9:100 was monitored. Then, the slope factor under the

414 slope condition was obtained using Formula (10).

415 
$$S_{\theta} = \frac{A_{\theta}}{A}, \quad (10)$$

416 where  $S_{\theta}$  represents the slope factor when the slope is  $\theta$ ,  $A_{\theta}$  represents the soil erosion intensity  
417 when the slope is  $\theta$  (t/hm<sup>2</sup>), and  $A$  represents the soil erosion intensity when the slope is 9%  
418 (t/hm<sup>2</sup>). The three slope conditions (1:1.5, 1:1.0, and control slope 9:100) in the soil erosion  
419 monitoring experiment, combined with Formula (10), were used to calculate the slope factor  
420 values of the two slopes (1:1.5 and 1:1.0) under the 30 rainfall conditions. The average factors of  
421 the slopes under the 1:1.5 and 1:1.0 slope conditions were 7.28 and 14.49, respectively (Table 7).

422 After the slope design drawings were digitized by ArcGIS, the slope and length values of each  
423 artificial slope prediction unit were determined according to the design specifications. The slope  
424 length value of each artificial slope prediction unit was the horizontal projection length of the  
425 cement frame. The slope length of the six arris brick revetment was 0. Formulas (5), (6), (9), and  
426 (10), combined with the slope length factor and  $m_a$  and  $S_{\theta}$  values, were used to calculate the value  
427 of  $LS$  of each artificial slope prediction unit.

428 **Table 7.** Calculation results of slope factor

The time of the second rainfall	$S_{46}$	$S_{56}$
2014.06.05	7.23	14.52
2014.06.07	7.25	14.47
2014.06.17	7.25	14.41
2014.06.28	7.33	14.62
2014.07.01	7.28	14.57
2014.07.13	7.27	14.57
2014.07.20	7.28	14.52
2014.08.02	7.20	14.43
2014.08.12	7.23	14.46
2014.08.26	7.27	14.60
2014.08.29	7.24	14.44
2014.09.02	7.25	14.56
2014.09.04	7.33	14.72
2014.09.17	7.30	14.32
2014.09.20	7.28	14.49

2014.10.05	7.33	14.73
2015.07.04	7.23	14.36
2015.07.15	7.24	14.32
2015.07.24	7.17	14.15
2015.07.28	7.39	14.68
2015.08.13	7.28	14.47
2015.08.19	7.33	14.53
2015.08.26	7.35	14.47
2015.09.03	7.22	14.47
2015.09.12	7.28	14.47
2015.09.17	7.29	14.48
2015.09.25	7.28	14.47
2015.10.03	7.27	14.53
2015.10.08	7.36	14.71
2015.10.12	7.40	14.26
Average	7.28	14.49

429 *Note: Sxy represents the slope factor value simultaneously solved by erosion intensity values for monitoring plots*  
430 *numbered x and y.*

431

### 432 3.2.5 Cover and management practice factor

433 The *C*-factor after topography is an important factor that controls soil loss risk. In the RUSLE  
434 model, the *C*-factor has been used to reflect the effects of vegetation cover and management  
435 practices on the soil erosion rate ((Vander-Knijff et al., 2000; Prasannakumar et al., 2011;  
436 Alkharabsheh et al., 2013). It is defined as the loss ratio of soils from land cropped under specific  
437 conditions to the corresponding loss from clean-tilled and continuous fallow (Wischmeier and  
438 Smith, 1978). Due to the variety of land cover patterns with severe spatial and temporal variation,  
439 mainly in the watershed scale, data sets from satellite remote sensing were used to assess the *C*-  
440 factor (Vander-Knijff et al., 2000; Li et al., 2010; Chen et al., 2011; Alexakis et al., 2013). **Taking**  
441 **full advantage of the Normalized Difference Vegetation Index (NDVI) data, C is calculated**  
442 **according to the equation of Gutman and Ignatov (1998).** The formula is shown as (11). Then, the  
443 vegetation coverage data were corrected by selecting a sample plot every 2 km along the study  
444 area for investigation. The algorithm for calculating *f* is referred to Tan et al (2005). The formula  
445 is shown as (11). Finally, accurate vegetation coverage data were obtained (Figure 7). The *C* factor  
446 map of the soil erosion prediction unit in the slope catchment area is shown in Figure 8.

$$447 \quad C = 1 - \frac{NDVI - NDVI_{\min}}{NDVI_{\max} - NDVI_{\min}} \quad (11)$$

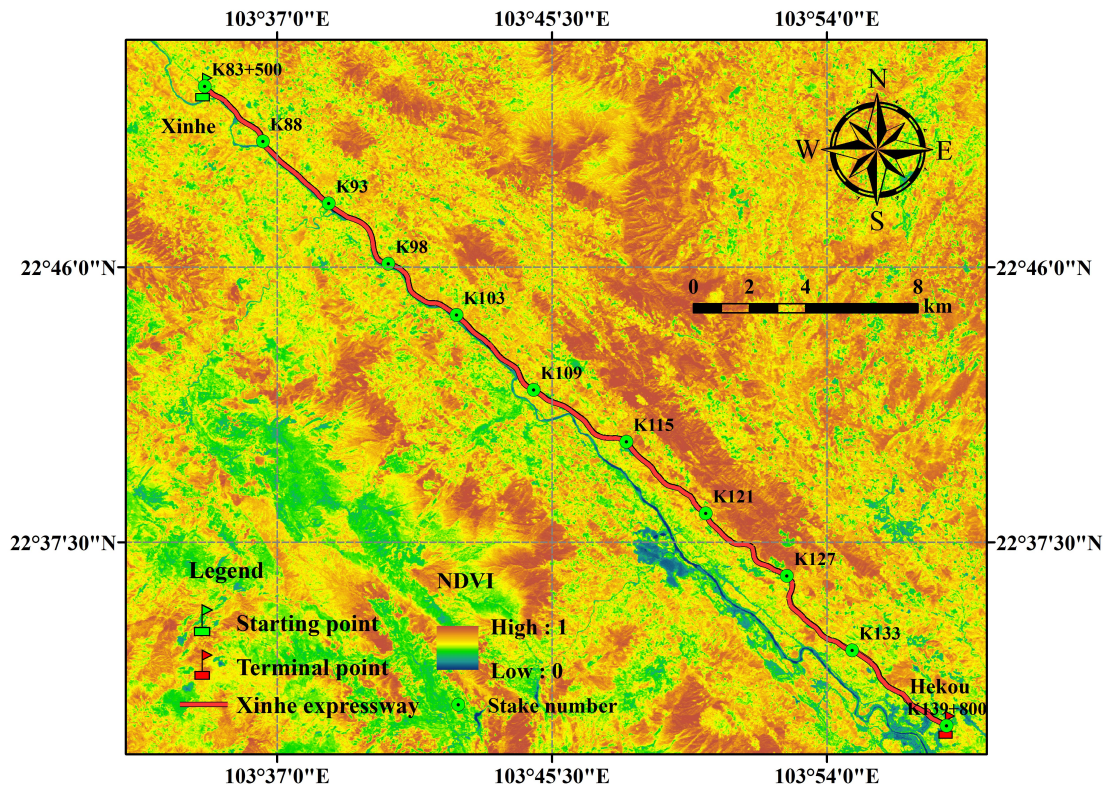


Figure 7. Vegetation coverage along Xinhe Expressway

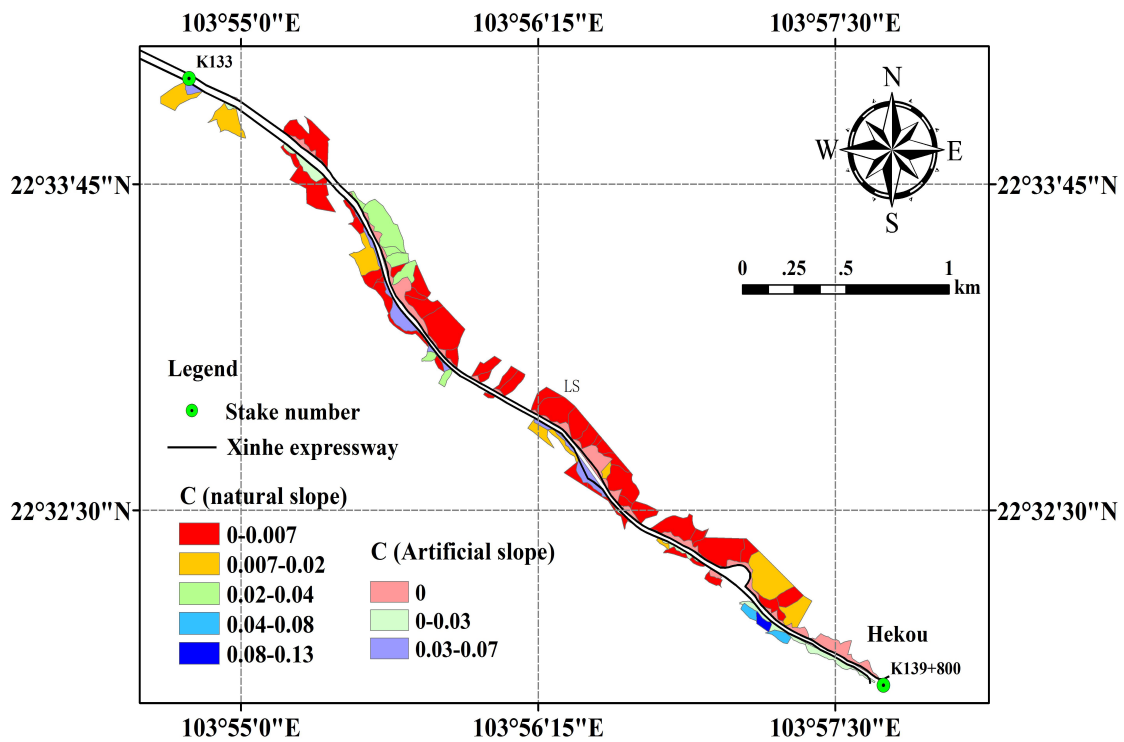


Figure 8. Spatial distribution map of cover and management practice factor

### 3.2.6 Factor of soil and water conservation measures

The land use types of the natural slope catchment area were mainly cultivated, forest,

456 construction, and difficult lands. Through field investigation and visual judgment, the water  
 457 conservation measures of the farmland and forestland were identified to be mainly contour belt  
 458 tillage, horizontal terrace and terrace, and artificial slope catchment area, including cement frame  
 459 and six arris brick revetments. The *P* values of the cement frame and the six arris brick revetments  
 460 were determined by the area ratio method as 0.85 and 0.4, respectively. The *P* values of the soil  
 461 and water conservation measures are shown in Table 8.

462 **Table 8.** *P* values of different slope types

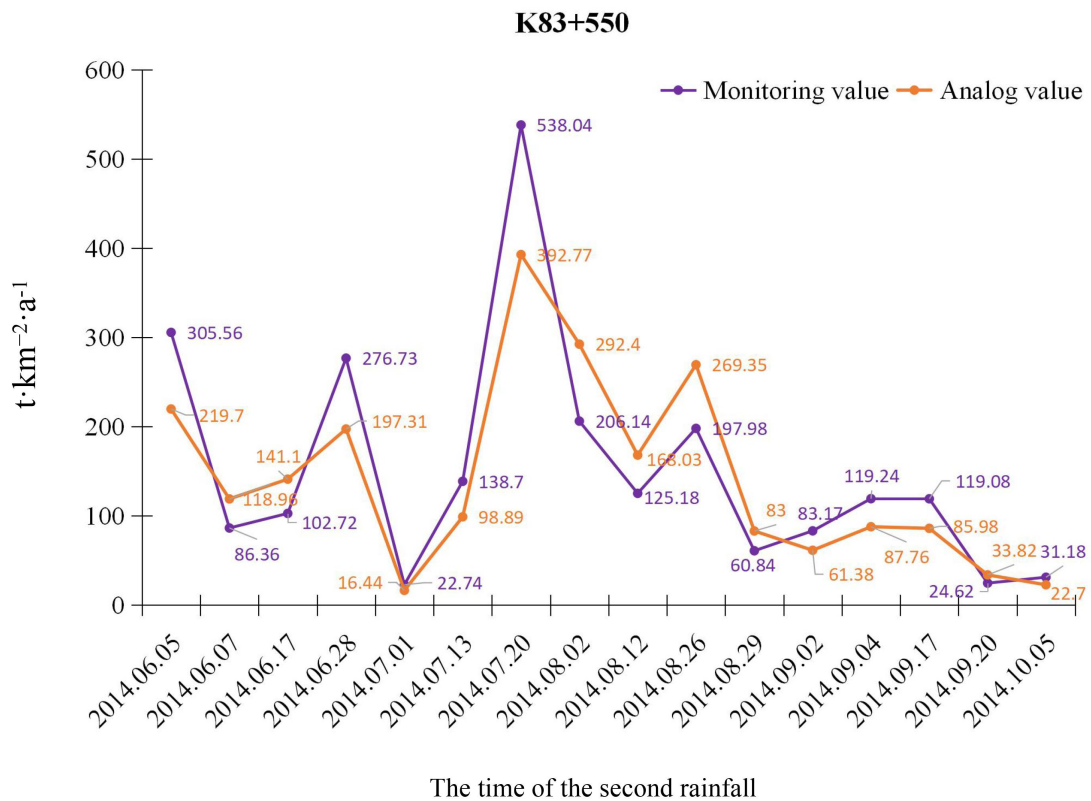
Slope type	Cement frame	Hexagonal brick	Contour strip tillage	Level bench/Terrace	Construction land	Difficult to use land	Other
<i>P</i>	0.85	0.4	0.55	0.03	0	0.2	1

463

464 **3.3 Validation of model simulation accuracy**

465 In this study, soil erosion in three monitoring areas under 16 erosive rainfall conditions was  
 466 monitored in 2014. No rainfall occurred in the 24 h preceding each rainfall, and the disturbance of  
 467 antecedent rainfall on soil erosion on the slopes was excluded. With an estimation of the historical  
 468 soil and water loss of each slope prediction unit, the results were compared with data from three  
 469 monitoring plots along the side slope of Xinhe Expressway, as shown in Figure 9-11.

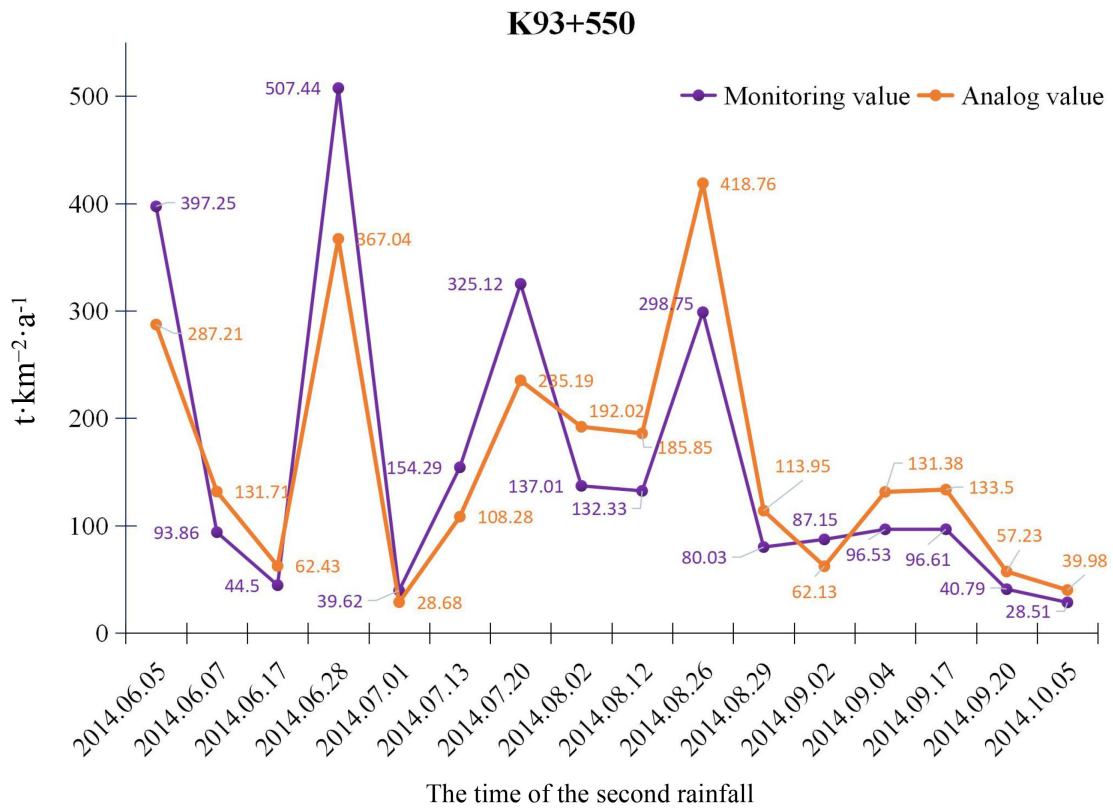
470



471

472

**Figure 9.** Comparison of model prediction and monitoring results (K83+550)

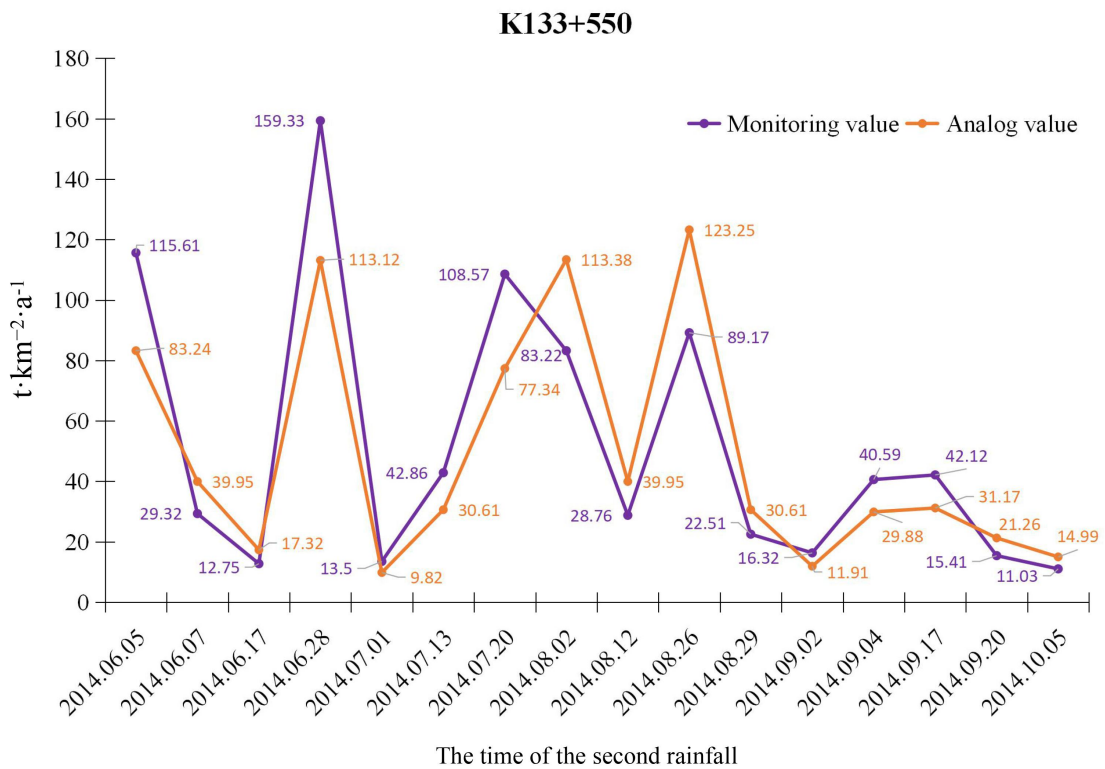


474

475

**Figure 10.** Comparison of model prediction and monitoring results ( K93+550)

476



477

478

**Figure 11.** Comparison of model prediction and monitoring results ( K133+550)

479

480

481 The error analysis shows that under the 16 rainfall conditions, the absolute errors of the  
482 three monitoring areas were 47.15, 52.52, and 16.27  $\text{t}\cdot\text{km}^{-2}\cdot\text{a}^{-1}$  and the overall average absolute  
483 error was 38.65  $\text{t}\cdot\text{km}^{-2}\cdot\text{a}^{-1}$ . The average relative errors were 31.80%, 35.49%, and 32.26%, and the  
484 overall mean relative error was 31.18%. The root mean square errors were 59.44, 65.64, and 20.95,  
485 all of which were within the acceptable range. The Nash efficiency coefficient of the model was  
486 0.67, which was between 0 and 1 and thus shows that the model accuracy satisfied the  
487 requirements. The calculation results are shown in Tables 10–12 (see the supplementary  
488 material/appendices).

488

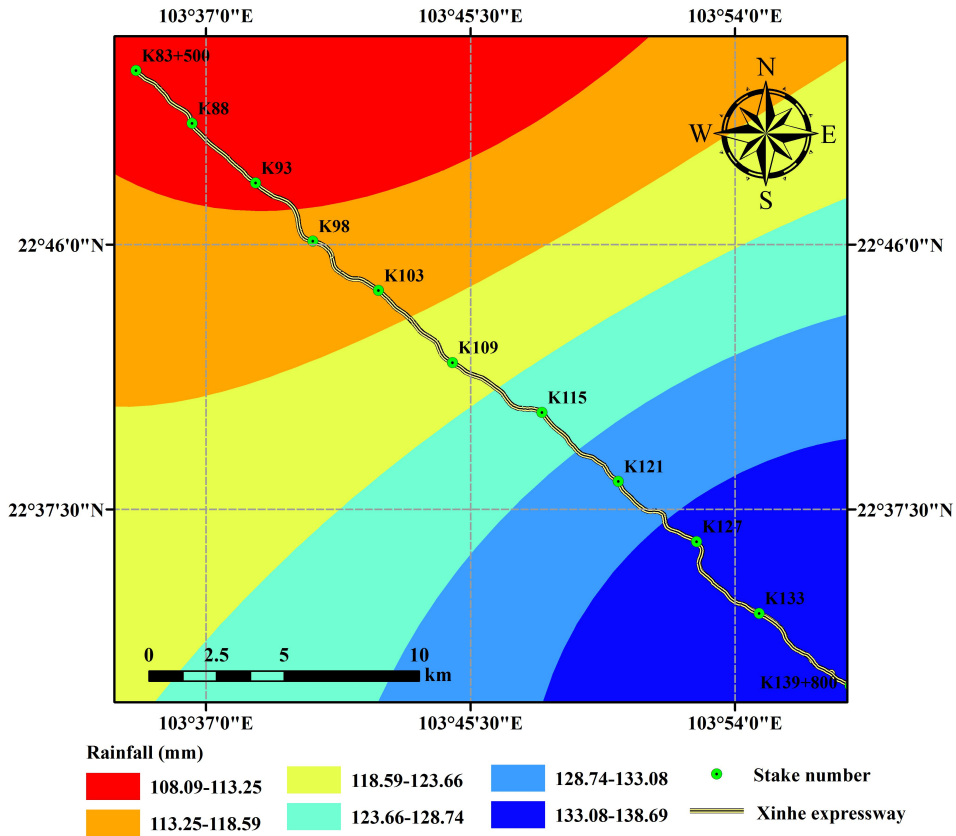
489 The analysis accuracy revealed that the northern and flat terrain of the southern region had a  
490 small simulation error due to the high and low areas of the central region of the terrain, which  
491 resulted in a slightly lower accuracy than that of the southern region. Under heavy rainfall  
492 conditions, the absolute error value of the simulation was large. On the one hand, the result may  
493 be caused by the artificial error in monitoring the sediment collection in the area. On the other  
494 hand, the model itself may be defective.

494

### 495 **3.4 Application of early warning of soil erosion to mountain expressway**

496

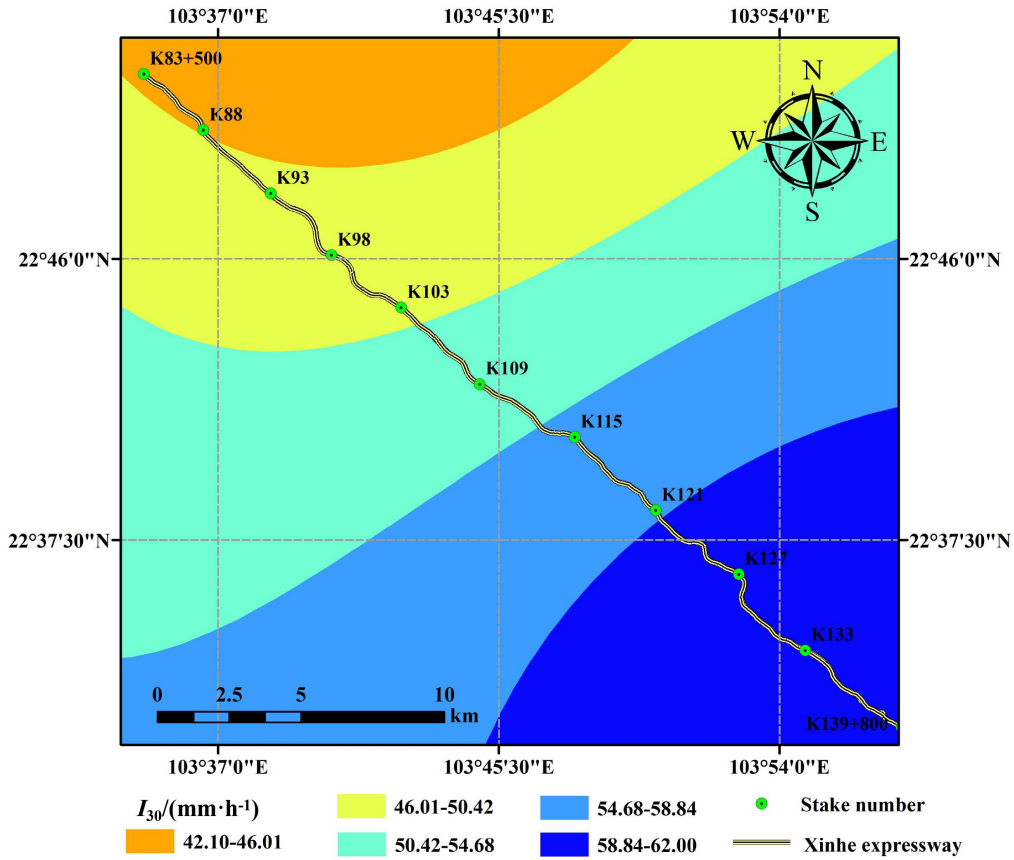
497 The rainfall data and  $I_{30}$  values in the 20 years covered by the study were obtained from the  
498 meteorological departments of Mengzi, Pingbian, Jinping, and Hekou counties in Yunnan  
499 Province. Rainfall and its intensity were interpolated using cokriging, which was introduced into  
elevation and geographical position, as shown in Figures 12 and 13.



500

501

Figure 12. Rainfall interpolation results under 20-year return



502

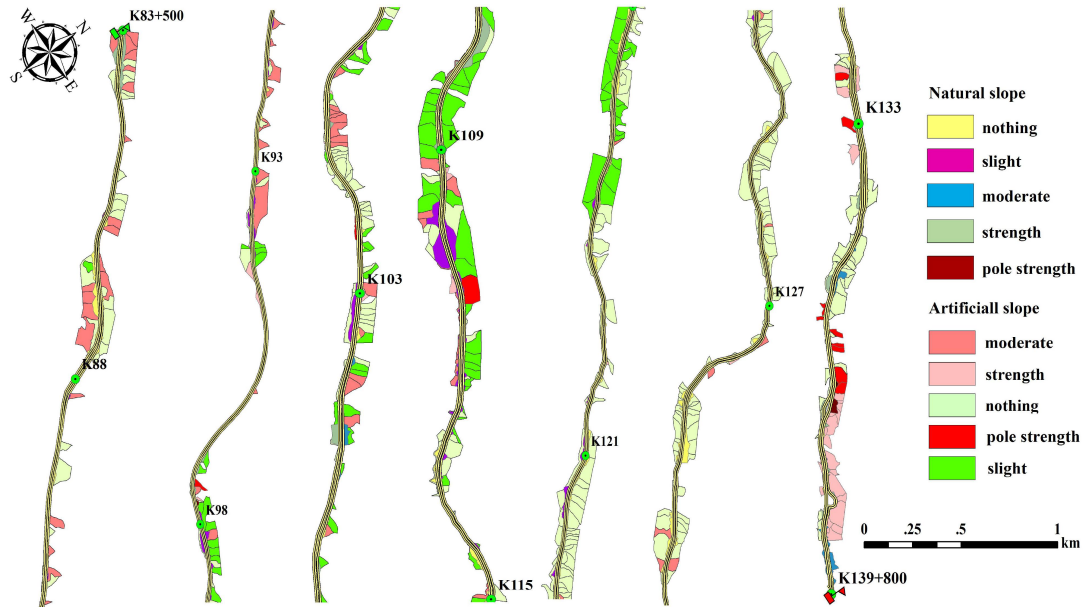
503

Figure 13. Rainfall intensity interpolation results under 20-year return



504

505 The total soil erosion amount of each prediction unit using 20-year rainfall data was obtained  
506 by simulation according to the soil erosion intensity classification standard. The prediction results  
507 were classified as “no risk,” “slight risk,” “moderate risk,” “high risk,” and “extremely high risk,”  
508 as shown in Figure 14.



509

510 **Figure 14.** Risk analysis of soil and water loss under 20-year rainfall conditions

511

512 The grading results showed that the percentage of prediction units classified under low and  
513 mild risk for soil and water loss was 88.60%. The risk of soil erosion was low in these areas. Thus,  
514 road traffic safety was not affected. The percentage of prediction units classified as having  
515 moderate risk was 4.29%. The risk of soil erosion in these areas was relatively low under the  
516 general rainfall intensity. However, under high rainfall intensity, a certain scale of soil erosion  
517 disaster could occur. The percentage of prediction units that were labeled high and extremely high  
518 risk was 7.11%. The risk of soil erosion was great in these units. For example, from K134+500 to  
519 K135+500 (1000 m), the average soil erosion amount on both sides of the slope under 20-year  
520 rainfall amount reached  $1757\text{t}\cdot\text{km}^{-2}\cdot\text{a}^{-1}$ . Even if only a portion of the sediment was deposited on  
521 the road, road safety would still be affected.

522 Similarly, the risk of soil erosion was analyzed according to the grading standard of soil and  
523 water loss risk under the condition of 20-year rainfall by simulating the soil erosion amount of  
524 each prediction unit under 1-year rainfall amount (Figure 15).

525

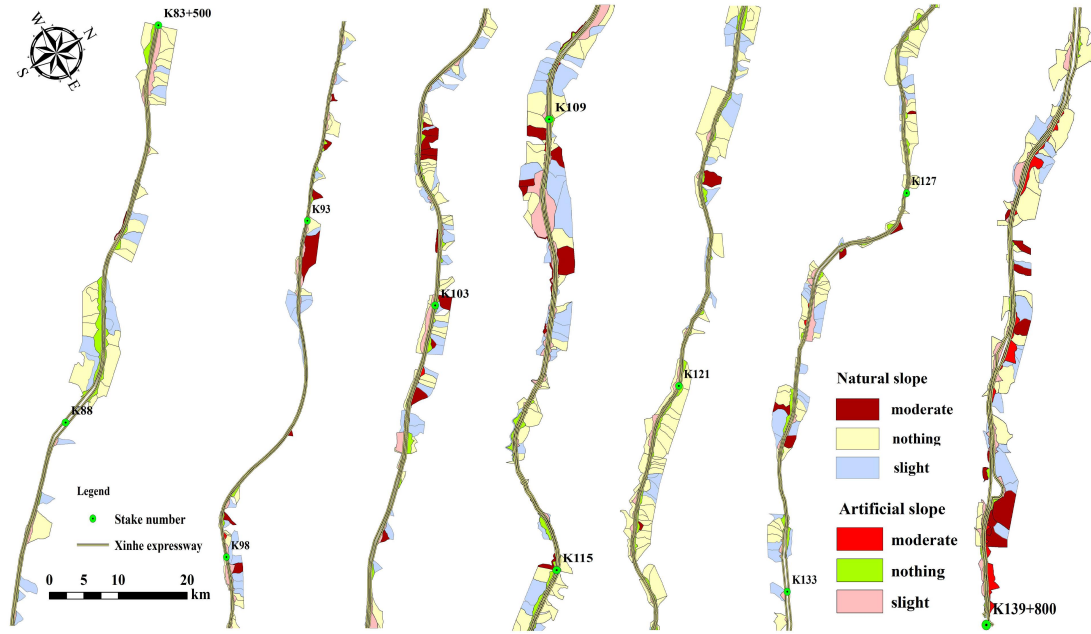


Figure 15. Risk analysis of soil and water loss under 1-year rainfall amount

The results indicated that the percentages of the prediction units with no and mild soil erosion risks were 78.00% and 17.92%, respectively. The risk of soil erosion was low in these areas. Thus, the safety of road traffic would not be affected. The percentage of prediction units at risk of mild soil erosion was 6.08%. The layout of soil and water conservation measures in these areas should therefore be rationally adjusted. Moreover, the comprehensive management of their slopes should be strengthened, and plant and engineering measures should be applied comprehensively to conserve soil and water in these regions. Inspections should be reinforced and motorists should be reminded to pay attention to traffic safety during the rainy season. Most of the artificial slopes covered by the study are made of six arris brick revetment, the amount of soil erosion is small, but the frame-type cement slope protection against soil erosion is sturdier than that in other areas. Slope protection measures should be rationally adjusted according to predicted results. We may consider slowing down the roadbed slope to keep the slope stable, then the ecological slope protection technology can be adopted. Such as the spraying and planting technology of bolt hanging net, it can build a layer of planting matrix which can grow and develop on the weathered rock slope, and can resist the porous and stable structure of the scouring. Finally, it can achieve the purpose of preventing and controlling soil erosion, beautifying the landscape environment of the road area and ensuring the safety of road traffic.

#### 4 Discussion

Slope is the main part of soil and water loss caused by highways. So, it is very important to predict and early warning. The highway slope is divided into natural slope and engineering (artificial) slope. The RUSLE model is used to predict the soil erosion of natural slope, on the

551 premise of not considering the variation in rainfall erosivity, it is found that in the same type area,  
552 the method of model parameters acquisition are basically consistent through the literature analysis  
553 and comparison (Yang 1999; Yang 2002; Peng et al., 2007; Zhao et al., 2007; Chen et al., 2014;  
554 Zhu et al., 2016), after comparing the monitoring data onto runoff plots, it is found that the error  
555 between the predicted value and the monitoring value calculated by the RUSLE model is small  
556 (Yang 1999; Yang 2002; Li et al., 2004), it shows that the prediction results of the model are  
557 reliable. In the prediction of slope erosion of engineering (artificial), the previous study mainly  
558 considered the disturbance to the surface during the construction process (He 2004; Liu et al.,  
559 2011; He 2008; Hu, 2016; Zhang et al., 2016; Song et al., 2007), and do not consider the soil  
560 erosion resulting from the construction of the engineering slope; In the process of predicting soil  
561 and water loss in engineering slope by using RUSLE model, the correction of the conservation  
562 support practice factor (such as cement block, hexagonal brick, etc.) will often be ignored (Zhang  
563 2011; Morschel et al., 2004; Correa and Cruz 2010); In addition, most of the cases using RUSLE  
564 model to predict soil erosion of highway slopes, in the use of remote sensing, it is usually based on  
565 grid data, but lack of consideration for catchment units (Islam et al., 2018; Villarreal et al., 2016;  
566 Wu and Yan 2014; Chen et al., 2010).

567 Therefore, this study analysis the characteristics of soil erosion in the process of expressway  
568 construction, and improves the following aspects on the basis of previous research: (1) In order to  
569 be closer to the actual situation, we divide the highway slope into natural unit and artificial unit,  
570 and calculate the amount of soil loss from the slope surface to the pavement by the slope surface  
571 catchment unit, which is more in line with the actual situation, and this idea can be popularized; (2)  
572 We consider the spatial heterogeneity of linear engineering of expressway, then the rainfall factor  
573 is spatially interpolated, it has made up for the defects of rainfall data usually used by rainfall  
574 stations in previous studies. (3) We modify the parameters of the artificial slope by means of  
575 actual survey, runoff plot observation and other means, and the parameters of the artificial slope  
576 are corrected by referring to the form of the project and the materials used.

577

## 578 **5 Conclusions**

579 This study fully considered the differences between the model parameters of the artificial and  
580 natural slopes of mountain expressways. Each catchment area was considered a unit. The artificial  
581 and natural slope prediction units were then divided, thus producing 422 artificial slope prediction  
582 units and 814 natural slope catchment prediction units. The soil and water loss of each slope was  
583 predicted in real time, thus making the prediction of soil erosion accurate. The  $R$  factor used the  
584 space interpolation method and the  $P$  factor of the artificial slope was corrected by the area ratio  
585 method in determining the parameters of model prediction. The other factors were corrected by the  
586 experimental data. Error analysis of the actual observation data revealed that the overall average  
587 absolute error of each monitoring area was  $38.65 \text{ t}\cdot\text{km}^{-2}\cdot\text{a}^{-1}$ , the average relative error was 31.18%,  
588 the root mean square error was between 20.95 and 65.64, and the Nash efficiency coefficient was  
589 0.67. The method of soil and water loss prediction adopted in this work generally has less error

590 and higher prediction accuracy than other models and can satisfy prediction requirements. The risk  
591 grades of the soil and water loss along the slope of Xinhe Expressway were divided into 20- and  
592 1-year rainfall on the basis of the simulated prediction. The results showed that the percentage of  
593 slope areas with high and extremely high risks was 7.11%. These areas were mainly in the  
594 K109+500–K110+500 and K133–K139+800 sections. Therefore, relevant departments should  
595 strengthen disaster prevention and reduction efforts and corresponding water and soil conservation  
596 initiatives in these areas.

597

## 598 **6 Acknowledgements**

599 This research work was supported jointly by the Yunnan Provincial Communications Department  
600 Project [2012-272-(1)] and the Yunnan Provincial Science and Technology Commission Project  
601 (2014RA074).

602

## 603 **7 References**

- 604 Alexakis, D., Diofantos, G., Hadjimitsis, A.: Integrated use of remote sensing, GIS and  
605 precipitation data for the assessment of soil erosion rate in the catchment area of “Yialias” in  
606 Cyprus. *Atmospheric Research*, 131, 108-124, 2013.
- 607 Alkharabsheh, M.M., Alexandridis, T.K., Bilasb, G., Misopolinos, N.: Impact of land cover  
608 change on soil erosion hazard in northern Jordan using remote sensing and GIS. Four decades  
609 of progress in monitoring and modeling of processes in the soil-plant-atmosphere system:  
610 applications and challenges. *Procedia Environmental Science*, 19, 912-921, 2013.
- 611 Angulomartínez, M., and Beguería, S.: Estimating rainfall erosivity from daily precipitation  
612 records: a comparison among methods using data from the ebro basin (NE Spain). *Journal of*  
613 *Hydrology*, 379(1): 111-121, 2009.
- 614 Bakr, N., Weindorf, D. C., Zhu, Y. D., Arceneaux, A. E., Selim, H. M.: Evaluation of  
615 compost/mulch as highway embankment erosion control in Louisiana at the plotscale. *Journal*  
616 *of Hydrology*, 468-469(6): 257-267, 2012.
- 617 Bosco, C., De Rigo, D., Dewitte, O., Poesen, J., and Panagos, P.: Modelling soil erosion at  
618 European scale: towards harmonization and reproducibility. *Natural Hazards & Earth System*  
619 *Sciences*, 2(4), 2639-2680, 2015.
- 620 Cai, C. F., Ding, S. W., Shi, Z. H., Huang, L., Zhang, G. Y.: Study of Applying USLE and  
621 Geographical Information System IDRISI to Predict Soil Erosion in Small Watershed.  
622 *Journal of Soil and Water Conservation*. 14(2): 19-24, 2000.
- 623 Chen, B. H.: The study on multivariate spatial interpolation method of precipitation in  
624 mountainous areas. Beijing Forestry University, 2016 (in Chinese).
- 625 Chen, F., Zeng, M. G., and Zhou, Z. H.: Evaluation for Ecological Benefits of Greening on  
626 Expressways in Mountainous Area. *Technology of Highway and Transport*, 1:139-143, 2015  
627 (in Chinese).
- 628 **Chen, S. X., Yang, X. H., Xiao, L. L., Cai, Y. H.: Study of Soil Erosion in the Southern Hillside**  
629 **Area of China Based on RUSLE Model. *Resources Science*, 36(6): 1288-1297, 2014 (in**  
630 **Chinese).**

631 Chen, T., Niu, R. Q., Li, P. X., Zhang, L. P., Du, B.: Regional soil erosion risk mapping using  
632 RUSLE, GIS, and remote sensing: a case study in miyun watershed, north china.  
633 Environmental Earth Sciences, 63(3), 533-541, 2011.

634 Chen, Y. J., Sun, K. M., and Zhao, Y.: Experiment on the effect of rule caused by slope angle on  
635 sand and runoff under the condition of ecological protected slope. Journal of Water Resources  
636 & Water Engineering, 21(4):55-59, 2010 (in Chinese).

637 Chen, Z. W., He, F., and Wang, J. J.: Revises of Terrain Factors of Roadbed Side Slope in  
638 Universal Soil Loss Equation. HIGHWAY, 12:180-185, 2010 (in Chinese).

639 Chen, Z. W., He, F., Wang, J. J.: Revises of Terrain Factor of Roadbed Side Slope in Universal  
640 Soil Loss Equation. HIGHWAY, (12):180-185, 2010 (in Chinese).

641 Correa, C. M. C., Cruz, J.: Real and estimative erosion through RUSLE from forest roads in  
642 undulated at heavily undulated relief. Revista Árvore, 34(4): 587-595, 2010.

643 Cunha, E. R. D., Bacani, V. M., Panachuki, E.: Modeling soil erosion using RUSLE and GIS in a  
644 watershed occupied by rural settlement in the Brazilian Cerrado. Natural Hazards, 85, 1-18,  
645 2017.

646 Dong, H., Zeng, H.: Discussion on the current situation and the future of China highway  
647 construction. Technology & Economy in Areas of Communication (TEAC), 5(3):17-18, 2003  
648 (in Chinese).

649 Fei, X. H., Song, Q. H., Zhang, Y. P., Liu, Y. T., Sha, L. Q., Yu, G. R., Zhang, L. M., Duan, C. Q.,  
650 Deng, Y., Wu, C. S., Lu, Z. Y., Luo, K., Chen, A. G., Xu, K., Liu, W. W., Huang, H., Jin, Y. Q.,  
651 Zhou, R. W., Grace, J.: Carbon exchanges and their responses to temperature and  
652 precipitation in forest ecosystems in Yunnan, Southwest China. Science of The Total  
653 Environment, 616: 824-840, 2017.

654 Feng, Q., and Zhao, W. W.: The study on cover-management factor in USLE and RUSLE: a  
655 review. ACTA ECOLOGICA SINICA, 34(16):4461-4472, 2014 (in Chinese).

656 Fenta, A. A., Yasuda, H., Shimizu, K., Haregeweyn, N., and Negussie, A.: Dynamics of Soil  
657 Erosion as Influenced by Watershed Management Practices: A Case Study of the Agula  
658 Watershed in the Semi-Arid Highlands of Northern Ethiopia. Environmental Management,  
659 58(5): 1-17, 2016.

660 Foster, G. R., Weesies, G. A., McCool, D. K., Joder, D. C., Renard, K. G.: Revised Universal Soil  
661 Loss Equation User's Manual. Gov. Print. Office, Washington D.C. (48p), 1999.

662 Gong, J., and Yang, P.: Study on the Layout of Soil and Water Conservation Monitoring Sites  
663 during the Construction of Mountain Highways-Case Study of Enlai, Enqian Highway.  
664 Subtropical Soil and Water Conservation, 28(1):9-11, 2016 (in Chinese).

665 He, F.: Prediction of soil erosion in foundation slope of South Hubei Road Based on RUSLE.  
666 Beijing Normal University, 2008 (in Chinese).

667 He, X. W.: Study on prediction of soil erosion in Road area. Beijing Normal University, 2004 (in  
668 Chinese).

669 Hu, L.: Study on development and mechanism of water Erosion and Ecological water erosion  
670 control technology of Highway slope in Cold Region. Xi'an University of technology, 2016  
671 (in Chinese).

672 Islam, M. R., Wan, Z. W. J., Lai, S. H., Osman, N., Din, M. A. M., Zuki, F. M.: Soil erosion  
673 assessment on hillslope of GCE using RUSLE model. Journal of Earth System Science,

674 127(4): 50, 2018.

675 Jia, Z. R., Guo, and Z. Y.: Quantifying Evaluation Approach to Highway Soil Bioengineering.  
676 Research of Soil and Water Conservation, 15(2):260-262, 2008 (in Chinese).

677 Jiang, M., Pan, X. Y., Nie, W. T.: Preliminary analysis of prevention and control of soil and water  
678 loss in expressway project construction. Yangtze River, 48(12):61-64, 2017 (in Chinese).

679 Kateb, H. E., Zhang, H. F., Zhang, P. C., Mosandl, R. Soil erosion and surface runoff on different  
680 vegetation covers and slope gradients: A field experiment in Southern Shaanxi Province,  
681 China. Catena, 105(5): 1-10, 2013.

682 Kateb, H. E., Zhang, H. F., Zhang, P. C., Mosandl, R. Soil erosion and surface runoff on different  
683 vegetation covers and slope gradients: A field experiment in Southern Shaanxi Province,  
684 China. Catena, 105(5): 1-10, 2013.

685 Kinnell, P. I. A.: Applying the RUSLE and the USLE-M on hillslopes where runoff production  
686 during an erosion event is spatially variable. Journal of Hydrology, 519:3328-3337, 2014.

687 Li, H., Chen, X. L., Kyoung, J. L., Cai, X. B., Myung S.: Assessment of soil erosion and sediment  
688 Li, J. G., Dao, H. Y., Zhang, L., Zhang, H. K.: Soil and Water Loss Monitoring in the Dianchi  
689 Watershed. Research of Soil and Water Conservation, 11(2): 75-77, 2004 (in Chinese).

690 Lin, H. L., Zheng, S. T., and Wang, X. L.: Soil erosion assessment based on the RUSLE model in  
691 the Three-Rivers Headwaters area, Qinghai-Tibetan Plateau, China. ACTA  
692 PRATAICULTURAE SINICA, 26(7):11-22, 2017 (in Chinese)

693 Liu, B. Y., Nearing, M. A., Shi, P. J., and Jia, Z. W.: Slope length effects on soil loss for steep  
694 slopes. Soil Science Society of America Journal 64(5): 1759-1763, 2000.

695 Liu, S. L., Zhang, Z. L., Zhao, Q. H., Deng, L., Dong, S. K.: Effects of Road on Landscape Pattern  
696 and Soil Erosion: A Case Study of Fengqing County, Southwest China. Chinese Journal of  
697 Soil Science, 42(1): 169-173, 2011 (in Chinese).

698 Liu, W. Y.: Preliminary Study on R Index of Zhaotong Basin. Yunnan Forestry Science and  
699 Technology, (2):24-26, 1999 (in Chinese)

700 Liu, X. Y.: Study on the slope stability and its rheological influence in Mountain highway. Central  
701 South University, 2013 (in Chinese).

702 Mccool, D. K., Brown, L. C., Foster, G. R., Mutchler, C. K., and Meyer, L. D.: Revised slope  
703 steepness factor for the universal soil loss equation. Transactions of the ASAE-American  
704 Society of Agricultural Engineers (USA), 30(5): 1387-1396, 1987.

705 Millward, A. A., and Mersey, J. E.: Adapting the rusle to model soil erosion potential in a  
706 mountainous tropical watershed. Catena 38(2):109-129, 1999.

707 Molla, T., and Sisheber, B.: Estimating soil erosion risk and evaluating erosion control measures  
708 for soil conservation planning at Koga watershed in the highlands of Ethiopia. Solid Earth, 8,  
709 1-23, 2017

710 Moore, I. D., and Burch, G. J.: Physical basis of the length-slope factor in the universal soil loss  
711 equation. Soil Science Society of America Journal, 50(5): 1294-1298, 1986.

712 Mori, A., Subramanian, S. S., Ishikawa, T., Komatsu, M. A Case Study of a Cut Slope Failure  
713 Influenced by Snowmelt and Rainfall. Procedia Engineering, 189: 533-538, 2017.

714 Mori, A., Subramanian, S. S., Ishikawa, T., Komatsu, M. A Case Study of a Cut Slope Failure  
715 Influenced by Snowmelt and Rainfall. Procedia Engineering, 189: 533-538, 2017.

716 Morschel, J., Fox, D. M., & Bruno, J. F.: Limiting sediment deposition on roadways: topographic

717 controls on vulnerable roads and cost analysis of planting grass buffer strips. *Environmental*  
718 *Science & Policy*, 7(1): 39-45, 2004.

719 Mountain Region of Yunnan Province. *SCIENTIA GEOGRAPHICA SINICA*, 19(3):265-270,  
720 1999 (in Chinese)

721 Panagos, P., Ballabio, C., Borrelli, P., Meusburger, K., Klik, A., Rousseva, S., Tadić, M.P.,  
722 Michaelides, S., Hrabalíková, M., Olsen, P., Aalto, J., Lakatos, M., Rymaszewicz, A.,  
723 Dumitrescu, A., Beguería, S., Alewell, C.: Rainfall erosivity in Europe. *Science of the Total*  
724 *Environment*, 511:801-814, 2015.

725 Panagos, P., Borrelli, P., Meusburger, K., Yu, B., Klik, A., Lim, K.J., Yang, J.E., Ni, J., Miao, C.,  
726 Chattopadhyay, N., Sadeghi, S.H., Hazbavi, Z., Zabihi, M., Larionov, G.A., Krasnov, S.F.,  
727 Gorobets, A.V., Levi, Y., Erpul, G., Birkel, C., Hoyos, N., Naipal, V., Oliveira, P.T.S., Bonilla,  
728 C.A., Meddi, M., Nel, W., Al Dashti, H., Boni, M., Diodato, N., Van Oost, K., Nearing, M.,  
729 Ballabio, C. Global rainfall erosivity assessment based on high-temporal resolution rainfall  
730 records. *Scientific Reports*, 7(1): 4175, 2017.

731 Panagos, P., Standardi, G., Borrelli, P., Lugato, E., Montanarella, L., Bosello, F.: Cost of  
732 agricultural productivity loss due to soil erosion in the European union: from direct cost  
733 evaluation approaches to the use of macroeconomic models. *Land Degradation &*  
734 *Development*. 2018.

735 Panos, P., Cristiano, B., Pasquale, B., Katrin, M., Andreas, K., Svetla, R., Melita, P. T., Silas, M.,  
736 Michaela, H., Preben, O., Juha, A., Mónica, L., Anna, R., Alexandru, D., Santiago, B., and  
737 Christine, A.: Rainfall erosivity in Europe. *Science of the Total Environment*, 511: 801, 2015.

738 Peng, J., Li, D. D., Zhang, Y. Q.: Analysis of Spatial Characteristics of Soil Erosion in Mountain  
739 Areas of Northwestern Yunnan Based on GIS and RUSLE. *Journal of mountain science*,  
740 25(5): 548-556, 2007 (in Chinese).

741 Prasannakumar, R., Shiny, N., Geetha, H., Vijith, H.: Spatial prediction of soil erosion risk by  
742 remote sensing, GIS and RUSLE approach: a case study of Siruvani river watershed in  
743 Attapady valley, Kerala, India. *Environmental Earth Science*, 965-972, 2011.

744 Renard, K. G., Foster, G. R., Weesies, G. A., McCool, D. K., and Yoder, D. C.: Predicting soil  
745 erosion by water: a guide to conservation planning with the revised universal soil loss  
746 equation (RUSLE). *Agriculture Handbook*, 1997.

747 Renard, K. G., Foster, G. R., Weesies, G. A., McCool, D. K., Yoder, D. C.: Predicting soil erosion  
748 by water-a guide to conservation planning with the Revised Universal Soil Loss Equation  
749 (RUSLE). *United States Department of Agriculture, Agricultural Research Service (USDA-*  
750 *ARS) Handbook No.703. United States Government Printing Office: Washington, DC. 1997.*

751 Rick, D., Van, R., Matthew, E. H., and Robert J. H.: Estimating the LS Factor for RUSLE through  
752 Iterative Slope Length Processing of Digital Elevation Data within ArcInfo Grid. *Cartography*,  
753 30(1): 27-35, 2001.

754 Shamshad, A., Azhari, M. N., Isa, M. H., Hussin, W. M. A. W., and Parida, B. P.: Development of  
755 an appropriate procedure for estimation of RUSLE EI<sub>30</sub> index and preparation of erosivity  
756 maps for Pulau Penang in Peninsular Malaysia. *Catena*, 72(3): 423-432, 2008.

757 Sharpley, A. N., and Williams, J. R.: EPIC-erosion/productivity impact calculator: 2. User manual.

758 Technical Bulletin-United States Department of Agriculture, 4(4): 206-207, 1990.

759 Shi, Z. H., Cai, C. F., Ding, S. W., Wang, T. W., and Chow, T. L.: Soil conservation planning at the  
760 small watershed level using RUSLE with GIS: a case study in the three gorge area of china.  
761 *Catena*, 55(1): 33-48, 2004.

762 Shu, Z. Y., Wang, J. Y., Gong, W., Lv, X. N., Yan, S Y., Cai, Y., Zhao, C. P.: Effects of compound  
763 management in citrus orchard on soil micro-aggregate fractal features and soil physical and  
764 chemical properties. *Journal of Nanjing Forestry University (Natural Sciences Edition)*, 41(5):  
765 92-98, 2017.

766 Silburn, D. M.: Hillslope runoff and erosion on duplex soils in grazing lands in semi-arid central  
767 Queensland. III. USLE erodibility (K factors) and cover-soil loss relationships. *Soil Research*,  
768 49(49): 127-134, 2011.

769 **Soil and Water Conservation Society. RUSLE user's guide. Soil and Water Cons. Soc. Ankeny, IA.**  
770 **164pp, 1993.**

771 Song, F. L., Ma, Y. H., Zhang, C. X., Yu, H. M., Hu, H. X., He, J. L., Huang, J. Y.: Research  
772 progress on greening substrate material of ecological protection of expressway-side slope.  
773 *Science of Soil and Water Conservation*, 6:57-61, 2008 (in Chinese).

774 **Song, X. Q., Zhang, C. Y., Liu, J.: Formation of Soil and Water Loss and Its Characteristics in**  
775 **Development and Construction Projects. *Bulletin of Soil and Water Conservation*, 27(5): 108-**  
776 **113, 2007 (in Chinese).**

777 Stanchi, S., Freppaz, M., Ceaglio, E., Maggioni, M., Meusburger, K., & Alewell, C., and Zanini,  
778 E.: Soil erosion in an avalanche release site (Valle d'Aosta: Italy): towards a winter factor for  
779 RUSLE in the Alps. *Natural Hazards & Earth System Sciences*, 14(7), 255-440, 2014.

780 Tan, B. X., Li, Z. Y., Wang, Y .H., Yu, P. T., Liu, L. B.: Estimation of Vegetation Coverage and  
781 Analysis of Soil Erosion Using Remote Sensing Data for Guishuihe Drainage Basin. *Remote*  
782 *sensing technology and application*. 20 (2): 215-220, 2005.

783 Tan, S. H., and Wang, Y. M.: Research Progress and Thinking of Bioengineering Techniques for  
784 Slope Protection in Expressway. *Research of Soil and Water Conservation*, 11(3):81-84, 2004  
785 (in Chinese).

786 **Taye, G., Vanmaercke, M., Poesen, J., Wesemael, B. V., Tesfaye, S., Teka, D., et al.: Determining**  
787 **RUSLE P-and C-factors for stone bunds and trenches in rangeland and cropland, North**  
788 **Ethiopia. *Land Degradation & Development*, 29(5), 2017.**

789 **Toy, T. J., Foster, G. R., Renard, K. G.: Soil Erosion: Processes, Prediction, Measurement, and**  
790 **Control. 2002**

791 Tresch, S., Meusburger, K., and Alewell, C.: Influence of slope steepness on soil erosion  
792 modelling with RUSLE, measured with rainfall simulations on subalpine slopes. *Bulletin of*  
793 *Hokkaido Prefectural Agricultural Experiment Stations*, 1995.

794 Vander-Knijff, J.M., Jones, R.J.A., Montanarella, L.: Soil Erosion Risk Assessment in Europe  
795 EUR 19044 EN. Office for Official Publications of the European Communities, Luxembourg.  
796 34, 2000.

797 **Villarreal, M. L., Webb, R. H., Norman, L. M., Psillas, J. L., Rosenberg, A. S., Carmichael, S.:**  
798 **Modeling landscape-scale erosion potential related to vehicle disturbances along the USA-**  
799 **Mexico border. *Land Degradation & Development*, 27(4): 1106-1121, 2016.**

800 **Wang, H. J., Yang, Y., and Wang, W. J.: Prediction of Soil Loss Quantity on Side Slope of Freeway**



801 Construction: Amendments to Main Parameters of USLE. *Journal of Wuhan University of*  
802 *Technology (Transportation Science & Engineering)*, 29(1):12-15, 2005 (in Chinese).

803 Wang, K., and Gao, Z. L.: Analysis of Bioengineering Technology for Slope Protection of  
804 Expressway: Taking Expressway from Ankang to the Border of Shaanxi and Hubei as an  
805 Example. *Ecological Economy*, 31(5):155-159, 2015 (in Chinese).

806 Wang, L. H., Ma, B., and Wu, F. Q.: Effects of wheat stubble on runoff, infiltration, and erosion of  
807 farmland on the Loess Plateau, China, subjected to simulated rainfall. *Solid Earth*, 8(2), 1-28,  
808 2017.

809 Wang, W. Z., and Jiao, J. Y.: Quantitative Evaluation on Factors Influencing Soil Erosion in China.  
810 *Bulletin of Soil and Water Conservation*, (st):1-20, 1996 (in Chinese).

811 Wang, W. Z., and Zhang, X. K.: Distribution of Rainfall Erosivity  $R$  Value in China. *Journal of soil*  
812 *erosion and soil conservation*, 2(1): 7-18, 1995.

813 Wang, W. Z., Jiao, J. Y., Hao, X. P., Zhang, X. K., Lu, X. Q., Chen, F. Y., Wu, S. Y.: Study on  
814 Rainfall Erosivity in China. *Journal of Soil and Water Conservation*, (4):7-18, 1995 (in  
815 Chinese)

816 Wischmeier, W.H., Smith, D.D.: Predicting rainfall erosion losses: a guide to conservation  
817 planning. In: USDA, Agriculture Handbook No. 537, Washington, DC, 1978.

818 Wischmerie, W. H., and Smith, D. D.: Predicting rainfall-erosion losses from cropland east of the  
819 rocky mountains: a guide to conservation planning, 1965.

820 Wu, Y. L., Yan, L. J.: Impact of road on soil erosion risk pattern based on RUSLE and GIS: a case  
821 study of Hangjinqi highway, Zhuji section. *ACTA ECOLOGICA SINICA*, 34(19):5659-5669,  
822 2014 (in Chinese).

823 Xiao, P. Q., Shi, X. J., Chen, J. N., Wu, Q., Yang, J. F., Yang, C. X., and Wang, C. G.:  
824 Experimental Study on Protecting Speedway Slope Under Rainfall and Flow Scouring.  
825 *Bulletin of Soil and Water Conservation*, 24(1):16-18, 2004 (in Chinese).

826 Xu, X. L., Liu, W., Kong, Y. P., Zhang, K. L., Yu, B. F., Chen, J. D.: Runoff and water erosion on  
827 road side-slopes: Effects of rainfall characteristics and slope length. *Transportation Research*  
828 *Part D: Transport and Environment*, 14(7): 497-501, 2009.

829 Yang, X.: Deriving rusle cover factor from time-series fractional vegetation cover for hillslope  
830 erosion modelling in new south wales. *Soil Research*, 52(52): 253-261, 2014.

831 Yang, Y. C., Wang, M. Z., Xu, Y. Y., Wang, P. C., and Song, Z. P.: Prediction of Soil Erosion on  
832 Embankment Slope of Qinhuangdao-Shenyang Special Line for Passenger Trains. *Journal of*  
833 *Soil and Water Conservation*, 15(2):14-16, 2001(in Chinese).

834 Yang, Y., and Wang, K.: Discussions on the Side Slope Protection System For Expressway.  
835 *Industrial Safety and Environmental Protection*, 32(1):47-49, 2006 (in Chinese).

836 Yang, Z. S.: A Study on Erosive Force of Rainfall on Sloping Cultivated Land in the Northeast  
837 **Yang, Z. S.: Study on Soil Loss Equation in Jinsha River Basin of Yunnan Province. *Journal of***  
838 **mountain science**, 20: 3-11, 2002 (in Chinese).

839 **Yang, Z. S.: Study on Soil Loss Equation of Cultivated Slopeland in Northeast Mountain Region**  
840 **of Yunnan Province. *Bulletin of Soil and Water Conservation*, (1): 1-9, 1999 (in Chinese).**  
841 yield in Liao watershed, Jiangxi Province, China, using USLE, GIS, and RS. *Journal of Earth*  
842 *Science* 2 (6), 941-953, 2010

843 Yoder, D. C., Foster, G. R., Renard, K. G., Weesies, G. A., and Mccool, D. K.: C-factor  
844 calculations in RUSLE. American Society of Agricultural Engineers. Meeting (USA), 1993.

845 Yuan, C., Yu, Q. H., You, Y. H., Guo, L.: Deformation mechanism of an expressway embankment  
846 in warm and high ice content permafrost regions. *Applied Thermal Engineering* 121: 1032-  
847 1039, 2017.

848 Yuan, C., Yu, Q. H., You, Y. H., Guo, L.: Deformation mechanism of an expressway embankment  
849 in warm and high ice content permafrost regions. *Applied Thermal Engineering* 121: 1032-  
850 1039, 2017.

851 Yuan, J. P.: Preliminary Study on Grade Scale of Soil Erosion Intensity. *Bulletin of Soil and Water*  
852 *Conservation*, 19(6):54-57, 1999 (in Chinese).

853 Zeng, C., Wang, S. J., Bai, X. Y., Li, Y. B., Tian, Y. C., Li, Y., Wu, L. H., and Luo, G. J. : Soil  
854 erosion evolution and spatial correlation analysis in a typical karst geomorphology using  
855 RUSLE with GIS. *Solid Earth*, 8(4), 1-26, 2017.

856 Zerihun, M., Mohammedyasin, M. S., Sewnet, D., Adem, A. A., & Lakew, M.: Assessment of soil  
857 erosion using RUSLE, GIS and remote sensing in NW Ethiopia. *Geoderma Regional*,12: 83-  
858 90, 2018.

859 Zerihun, M., Mohammedyasin, M. S., Sewnet, D., Adem, A. A., Lakew, M.: Assessment of soil  
860 erosion using RUSLE, GIS and remote sensing in NW Ethiopia. *Geoderma Regional*, 12, 83-  
861 90, 2018.

862 Zhang, D. S.: The calculation of urban soil erosion based on GIS-a case study of Wuhan City.  
863 *Southwest University of M.S.Dissertation*, 2011 (in Chinese).

864 Zhang, H., Liao, X. L., Zhai, T. L.: Evaluation of ecosystem service based on scenario simulation  
865 of land use in Yunnan Province. *Physics and Chemistry of the Earth, Parts A/B/C*. 2017.

866 Zhang, T., Jin, D. G., Dong, G. C., Lin, J., Tang, P., Li, L. P.: Monitoring Soil Erosion in Linear  
867 Production and Construction Project Areas Based on RUSLE-A Case Study of North Ring  
868 Expressway in Ningbo City, Zhejiang Province. *Bulletin of Soil and Water Conservation*,  
869 36(5): 131-135, 2016 (in Chinese).

870 Zhang, T., Jin, D. G., Tong, G. C., Lin, J., Tang, P., Li, L. P.: Monitoring Soil Erosion in Linear  
871 Production and Construction Project Areas Based on RUSLE - A Case Study of North Ring  
872 Expressway in Ningbo City, Zhejiang Province. *Bulletin of Soil and Water Conservation*,  
873 36(5):131-135, 2016 (in Chinese).

874 Zhao, L., Yuan, G. L., Zhang, Y., He, B., Liu, Z. H., Wang, Z. Y., Li, J.: The Amount of Soil  
875 Erosion in Baoxiang Watershed of Dianchi Lake Based on GIS and USLE. *Bulletin of So il*  
876 *and Water Conservation*, 27(3): 42-46, 2007 (in Chinese).

877 Zhou, F. C.: Highway Slope Ecological Protection Against Erosion Mechanism and Control Effect  
878 Research. *Chongqing jiaotong university*, 2010 (in Chinese).

879 Zhou, R. G., Zhong, L. D., Zhao, N. L., Fang, J., Chai, H., Jian, Z., Wei, L., Li. B.: The  
880 Development and Practice of China Highway Capacity Research. *Transportation Research*  
881 *Procedia*, 15: 14-25, 2016.

882 Zhou, R. G., Zhong, L. D., Zhao, N. L., Fang, J., Chai, H., Jian, Z., Wei, L., Li. B.: The  
883 Development and Practice of China Highway Capacity Research. *Transportation Research*  
884 *Procedia*, 15: 14-25, 2016.

885 Zhu, J., Li, Y. M., Jiang, D. M.: A Study on Soil Erosion in Alpine and Gorge Region Based on

- 886           GIS and RUSLE Model-Taking Lushui County of Yunnan Province as an Example. *Bulletin*  
887           *of Soil and Water Conservation*, 36(3): 277-283, 2016 (in Chinese).
- 888       Zhu, S. Q., Lin, J. L., and Lin, W. L.: Preliminary Study on Effects of Expressway Construction on  
889       Side-Slope Soil Erosion in Mountainous Areas. *Resources Science*, 26(1):54-60, 2004 (in  
890       Chinese).
- 891       Zhuo, M. N., Li, D. Q., and Zheng, Y. J.: Study on Soil and Water Conservation Effect of  
892       Bioengineering Techniques for Slope Protection in Highway. *Journal of Soil and Water*  
893       *Conservation*, 20(1):164-167, 2006 (in Chinese).